Atmos. Chem. Phys. Discuss., 15, 34719–34763, 2015
www.atmos-chem-phys-discuss.net/15/34719/2015/
doi:10.5194/acpd-15-34719-2015

Atmospheric Chemistry and Physics Discussions

The importance of vehicle emissions as a source of atmospheric ammonia in the megacity of Shanghai

Y. H. Chang[1], Z. Zou[2], C. R. Deng[1,3], K. Huang[1], J. L. Collett Jr.[4], J. Lin[1], and G. S. Zhuang[1]

[1]Center for Atmospheric Chemistry Study, Department of Environmental Science and Engineering, Fudan University, Shanghai 200433, China
[2]Pudong New Area Environmental Monitoring Station, Shanghai 200135, China
[3]Shanghai Key Laboratory of Atmospheric Particle Pollution and Prevention (LAP[3]), Department of Environmental Science and Engineering, Fudan University, Shanghai 200433, China
[4]Department of Atmospheric Science, Colorado State University, Fort Collins, CO 80523, USA

Received: 1 December 2015 – Accepted: 2 December 2015 – Published: 10 December 2015

Correspondence to: C. R. Deng (congruideng@fudan.edu.cn)
and G. S. Zhuang (gzhuang@fudan.edu.cn)

Published by Copernicus Publications on behalf of the European Geosciences Union.

Abstract

Agricultural activities are a major source contributing to NH_3 emissions in Shanghai and most other regions of China; however, there is a long-standing and ongoing controversy regarding the contributions of vehicle-emitted NH_3 to the urban atmosphere. From April 2014 to April 2015, we conducted measurements of a wide range of gases (including NH_3) and the chemical properties of $PM_{2.5}$ at hourly resolution at a Shanghai urban supersite. This large dataset shows NH_3 pollution events, lasting several hours with concentrations four times the annual average of 5.3 $\mu g\,m^{-3}$, caused by the burning of crop residues in spring. There are also generally higher NH_3 concentrations (mean $\pm 1\sigma$) in summer ($7.3 \pm 4.9\,\mu g\,m^{-3}$; $n = 2181$) because of intensive emissions from temperature-dependent agricultural sources. However, the NH_3 concentration in summer was only an average of 2.4 $\mu g\,m^{-3}$ or 41 % higher than the average NH_3 concentration of other seasons. Furthermore, the NH_3 concentration in winter ($5.0 \pm 3.7\,\mu g\,m^{-3}$; $n = 2113$) was similar to that in spring ($5.1 \pm 3.8\,\mu g\,m^{-3}$; $n = 2204$) but slightly higher, on average, than that in autumn ($4.5 \pm 2.3\,\mu g\,m^{-3}$; $n = 1949$). Moreover, other meteorological parameters like planetary boundary layer height and relative humidity were not major factors affecting seasonal NH_3 concentrations. These findings suggest that there may be some climate-independent NH_3 sources present in the Shanghai urban area. Independent of season, the concentrations of both NH_3 and CO present a marked bimodal diurnal profile, with maxima in the morning and the evening. A spatial analysis suggests that elevated concentrations of NH_3 are often associated with transport from regions west-northwest and east-southeast of the city, areas with dense road systems. The spatial origin of NH_3 and the diurnal concentration profile together suggest the importance of vehicle-derived NH_3 associated with daily commuting in the urban environment. To further examine vehicular NH_3 emissions and transport, sampling of the NH_3 concentration was performed in (from the entrance to the exit of the tunnel) and out (along a roadside transect spanning 310 m perpendicular to the tunnel) of a heavily trafficked urban tunnel during the spring 2014. NH_3 concentrations

ACPD
15, 34719–34763, 2015

in the tunnel exit were over 5 and 11 times higher than those in the tunnel entrance and in the ambient air, respectively. Based on the derived mileage-based NH_3 emission factor of 28 mg km^{-1}, a population of 3.04 million vehicles in Shanghai produced around 1300 t NH_3 in 2014, which accounts for 12 % of total NH_3 emissions in the urban area. Collectively, our results clearly show that vehicle emissions associated with combustion are an important NH_3 source in Shanghai urban areas and may have potential implications for $PM_{2.5}$ pollution in the urban atmosphere.

1 Introduction

Ammonia (NH_3) is one of the most abundant nitrogen-containing substances and the principal reduced nitrogen component in the atmosphere. It plays a strong role in local and regional scale tropospheric chemistry and air quality by serving as a precursor to particulate ammonium (pNH_4^+) (Seinfeld and Pandis, 2012). Although major efforts have been made towards regulating NO_x and SO_2 emissions to improve air quality in China (Wang et al., 2014; Zhao et al., 2013), a major portion of the nation's population presently lives in environments of non-compliance with national standards for fine particulate matter ($PM_{2.5}$, representing particles with aerodynamic diameters smaller than 2.5 microns) (Huang et al., 2014; Lin et al., 2010; Ma et al., 2014, 2015). NH_3 emission reduction has been proposed as a cost-effective strategy to lower ambient $PM_{2.5}$ levels (Heald et al., 2012; Pinder et al., 2007; Wang et al., 2011, 2013; Ye et al., 2011). However, the emission sources of NH_3 and their relative contributions to ambient concentrations, especially in urban atmospheres, remain uncertain (Chang, 2014; Felix et al., 2014; Yao et al., 2013).

Emission sources of NH_3 have been previously reviewed (e.g., Asman et al., 1998; Reis et al., 2009; Sutton et al., 2008). Major sources include volatilization of N-containing fertilizers and excreta from animal husbandry, which together contribute over 80 % of total global NH_3 emissions (Bouwman et al., 1997; Clarisse et al., 2009; Olivier et al., 1998; Schlesinger and Hartley, 1992). Thus it is not surprising that previous

ACPD
15, 34719–34763, 2015

investigations of NH_3 emissions were mainly performed adjacent to dairy operations (Mount et al., 2002), animal housing (Gay et al., 2003), livestock facilities (Kawashima and Yonemura, 2001), slurry lagoons (Aneja et al., 2000), pit latrines (Rodhe et al., 2004), and croplands (Yan et al., 2003), where elevated levels of NH_3 are often observed. Varying significantly in time and space, biomass burning (including agricultural waste, savanna and forest fires) may contribute up to 12 % of the global NH_3 emissions flux (Behera et al., 2013; Lamarque et al., 2010). Despite the focus on ammonia sources is typical of agricultural and rural environments, a number of studies reveal that ambient NH_3 concentrations in urban areas can be comparable to (Cao et al., 2009; Stanier et al., 2012) or even higher than (Bettez et al., 2013; Meng et al., 2011; Singh and Kulshrestha, 2014) those in rural areas. These observations strongly suggest that there must be other non-agricultural NH_3 sources present in urban areas.

Starting in the 1980s, the introduction of three-way catalytic converters (TWCs) on automobiles dramatically mitigated pollutant emissions from vehicle tailpipes (Shelef and McCabe, 2000). An unwanted side effect of the use of TWCs for gasoline powered vehicles and selective catalytic reduction (SCR) for control of nitrogen oxides emissions from diesel powered vehicles, has been an increase in NH_3 emissions from motor vehicles, a significant source of non-agricultural NH_3 that has been documented directly through laboratory dynamometer studies (Durbin et al., 2002; Heeb et al., 2008, 2006; Huai et al., 2005; Livingston et al., 2009; Suarez-Bertoa et al., 2014, 2015) and on-road measurements (including mobile chase systems and tunnel tests) (Brito et al., 2013; Fraser and Cass, 1998; Kean et al., 2009; Liu et al., 2014; Moeckli et al., 1996; Pierson and Brachaczek, 1983; Pierson et al., 1996; Sun et al., 2014), or indirectly through correlation analysis between ambient NH_3 concentrations and other recognized traffic tracers (e.g., CO, NO_x) (Bishop and Stedman, 2015; Gong et al., 2011, 2013; Ianniello et al., 2010; Nowak et al., 2010; Pandolfi et al., 2012; Phan et al., 2013; Reche et al., 2012). In the US, it is estimated that 5 % of the national NH_3 emissions are due to motor vehicles (Kean et al., 2009), while this figure is estimated at 12 % for the UK (Sutton et al., 2000), with almost all the remaining NH_3 coming from agricultural processes. At

ACPD
15, 34719–34763, 2015

a regional level, motor vehicle emissions make a small contribution to the total. Nevertheless, they are locally concentrated in urban areas where agricultural sources of NH_3 are mostly absent. Therefore, a disproportionately greater impact of motor vehicles on the urban NH_3 budget and subsequent secondary $PM_{2.5}$ formation can be expected (Chang, 2014). On the other hand, we notice that several important studies did not detect evidence of an influence of on-road traffic on ambient NH_3 concentrations (Pryor et al., 2004; Saylor et al., 2010; Yao et al., 2013). Therefore, more efforts needed to be made to elucidate the contribution of vehicle-emitted NH_3 to the urban atmosphere.

Shanghai, like many other cities in eastern China, is suffering severe air pollution problems, such as high $PM_{2.5}$ concentrations and resulting poor visibility (Huang et al., 2013b, 2012). Although there are many studies aimed at understanding PM pollution, little is known about the characteristics of NH_3 in the largest city of China. In an effort to curb its severe air pollution, China recently launched an air pollution monitoring research program (known as the supersite program) in several major cities. In 2014, a new in situ atmospheric station equipped with state-of-the-art instruments was installed in the Shanghai region, allowing comprehensive characterization of $PM_{2.5}$ and associated precursor gases. Here seasonal trends, diurnal variations and pollution episodes retrieved from one year of real-time measurement of NH_3 are presented and interpreted in order to explore the sources and parameters controlling the NH_3 concentrations across Shanghai. Meanwhile, an additional source-specific campaign was performed to examine the emission and transport of vehicle-emitted NH_3 from an urban heavily trafficked tunnel in Shanghai.

2 Methods

2.1 Long-term monitoring at Pudong supersite

In situ continuous observations of the chemical and optical properties of atmospheric aerosols and associated precursor gases were made on the rooftop (18 m a.g.l.) of

ACPD
15, 34719–34763, 2015

the Pudong Environmental Monitoring Center (PEMC; 121.5446° E, 31.2331° N), 5 km east of the Shanghai urban center (the People's Square) (Fig. 1). The site is located in a mixed-use urban area (office, commercial, residential and traffic) east of downtown Shanghai, with no obvious NH_3 point source within 5 km (Zou et al., 2015). As one of the state-controlled sites, Pudong (PD) supersite was designed by the Ministry of Environemtal Protection of China and operated by the Shanghai Environmental Monitoring Center, being responsible for the release of hourly air quality data for PM_{10}, $PM_{2.5}$, and other criteria pollutants (CO, SO_2, NO_x and O_3).

From 3 April 2014 to 2 April 2015, using a MARGA instrument (Measurement of Aerosols and Reactive Gases Analyzer, Metrohm Applikon B.V., NL), water-soluble gases (NH_3, HNO_3, HONO, HCl and SO_2) and $PM_{2.5}$ components (NO_3^-, Cl^-, SO_4^{2-}, Na^+, NH_4^+, K^+, Mg^{2+} and Ca^{2+}) were measured with hourly temporal resolution. The MARGA removes soluble gases in a rotating, wet-walled denuder, while a steam-jet aerosol collector is used for fine particle collection. Meanwhile, aerosol light absorption coefficients (b_{abs}) were retrieved every 5 min from an AE31 Aethalometer using seven wavelengths (370, 470, 520, 590, 660, 880 and 950 nm) with a $PM_{2.5}$ cut-off inlet. Black carbon (BC) concentrations for the whole data set were calculated from the absorption coefficient at 880 nm. The measurement process was subjected to rigorous quality assurance and quality control procedures according to the Technical Guideline of Automatic Stations of Ambient Air Quality in Shanghai based on the national specification HJ/T193-2005.

To explore the comparability between on-line and off-line methods for NH_3 measurement, an Ogawa passive sampling device (PSD) was co-located with MARGA at PD to passively measure weekly ambient NH_3 concentration from May 2014 to June 2015. The Ogawa PSD is a double-sided passive sampler equipped with two 14 mm quartz filters (serving as duplicates) impregnated with phosphoric acid provided by the manufacturer. Following the manufacturer's protocols (http://www.ogawausa.com), exposed filter samples were soaked with 8 mL ultra-pure water (18.2 MΩ cm) and analyzed by an ion chromatography system (883 Basic IC plus, Metrohm Co., Switzerland). The

ACPD
15, 34719–34763, 2015

detection limit for NH_4^+ in the passive sampler extracts was 2.8 µg L^{-1}; this corresponds to an ambient NH_3 concentration detection limit of approximately 0.1 ppb for a 7 day sample. The NH_3 concentrations measured by the MARGA (ppb) were averaged over the same time period as the Ogawa PSDs (ppb). Fig. S1 in the Supplement shows a good correlation ($y = 0.82 \times +0.56$, $n = 53$, $R^2 = 0.84$, $p < 0.001$) between the two NH_3 measurement methods, validating the reliability of NH_3 data from the MARGA platform.

2.2 On-road measurement of NH_3 concentration in and out of a tunnel

To complement the information obtained from the main monitoring campaign described above, additional measurements of NH_3 concentration were performed at eight sites in and out the Handan tunnel from 9 April to 21 May 2014. The Handan tunnel is a 720 m long urban freeway in the northeast of Shanghai, separating the campus of Fudan University into two parts (Fig. 9a). It contains an array of ventilation orifices in the middle section of the tunnel, 200 m in total. The tunnel has two traffic bores; each bore has a cross section of 70 m^2 and four lanes with typically 120 000 vehicles (of which 85 % of are light-duty vehicles) passing per day (Li, 2007). Driven by a group of high power fans, the average wind speed measured at the exit of the tunnel was approximately 5 ± 1 m s^{-1}. The maximum vehicle speed limit in the tunnel is 80 km h^{-1}, with typical driving speeds of 50–60 km h^{-1}. Inside the northern bore of the tunnel, four sampling points were located at both ends of the tunnel (10 m from the exit and entrance of the tunnel, or T-d and T-a, for short) and the two ends of an array of ventilation orifices located in the middle section of the tunnel (Fig. 9a; the site near the entrance and the exit named as T-b, and T-c for short, respectively). Outside the tunnel, a roadside transect involving four sites perpendicular to the tunnel was established, spanning the distance from 0 m ($O_{0\,m}$, for short), 20 m ($O_{20\,m}$), 150 m ($O_{150\,m}$), to 310 m ($O_{310\,m}$). Figure 9a shows the layout of the tunnel and the sampling points.

ACPD
15, 34719–34763, 2015

Using US EPA Method 207.1 (Determination of Ammonia Emissions from Stationary Sources), the NH_3 concentration at each site was measured. Briefly, for each sample, ambient air was pumped through two fritted glass bubblers (containing 10 mL 0.005 mol L^{-1} H_2SO_4 absorbing solution in each bubbler) for two hours at a flow rate of 1 L min^{-1}. These two bubblers were connected in series, and the NH_3 collection efficiency of the sampling trains was 95 % or better (checked by using four bubblers in series in our pilot study, the collection efficiency = 100× (the sum of the values of the first two bubblers)/the sum of the values of the four bubblers). Measurements were made during the morning (between 08:00 and 11:00 local time) and afternoon (between 14:00 and 19:00 LT). Due to the proximity of the monitoring sites to the laboratory, all samples could be collected and analyzed by IC swiftly to avoid potential contamination, and field blanks were below the detection limit. Due to the dangers to personnel of sampling at the T-a, T-b and T-c sites, six samples were collected synchronously at these three sites. 19 paired samples were successfully collected and determined at the site of T-d, $O_{0\,m}$, $O_{20\,m}$, $O_{150\,m}$ and $O_{310\,m}$.

2.3 Planetary boundary layer height simulation

The Weather Research and Forecasting (WRF) model v3.5.1 (Skamarock et al., 2008) is used for simulating the height of planetary boundary layer. The National Centers for Environmental Prediction (NCEP) Final (FNL) Operational Global Analysis dataset (http://rda.ucar.edu/datasets/ds083.2/) with a horizontal resolution of a resolution of 1.0° × 1.0° are incorporated as initial and boundary conditions for the model. An one-way nested approach with four-dimensional data assimilation (FDDA) in WRF is applied. The WRF model configurations can be found elsewhere (Huang et al., 2013a). A Meteorology/Chemistry Interface Processor (MCIP) (Otte and Pleim, 2010) v4.1 is used to postprocess the WRF output. The atmospheric height of the planetary boundary layer field, one of the standard MCIP outputs, is used in this study. Additionally, the planetary boundary layer depths at 3 h resolution were obtained from the US National Oceanic and Atmospheric Administration (NOAA) READY archived Global Data Assim-

ACPD
15, 34719–34763, 2015

ilation System (GDAS) meteorological data (1° × 1°) based on Coordinated Universal Time (UTC). All UTC values are converted to local time (UTC + 8).

2.4 Potential source contribution analysis

24 h back trajectories arriving at the PD supersite at a height of 500 m were calculated at 1 h time intervals for each of the four seasons using NOAA Hybrid Single-Particle Lagrangian Integrated Trajectory (HYSPLIT) model with GDAS one degree archive meteorological data (Draxler and Rolph, 1997). An in-depth back trajectory analysis, the potential source contribution function (PSCF), is useful for identifying the possible geographic origin of emission sources; this method calculates the ratio of the number of points with concentration higher than a threshold value (m_{ij}) to the total number of points (n_{ij}) in the ijth grid cell. Higher PSCF values indicate higher potential source contributions to the receptor site. In this study, the domain for the PSCF was set within the range of (26–42° N, 112.5–125.5° E) in 0.1° × 0.1° grid cells. The 75th percentile for CO and NH_3 during the four seasons was used as the threshold value m_{ij}. To reduce the uncertainties of m_{ij}/n_{ij} for those grid cells with a limited number of points, a weighting function recommended by (Polissar et al., 2001) was applied to the PSCF in each season. Visualizations of the PSCF were mapped using ArcMap 10.2.

3 Results and discussion

3.1 Temporal evolution of NH_3 concentrations

The temporal patterns of hourly gaseous NH_3 concentrations determined by the MARGA at the Pudong supersite are reported in Fig. 2. Summary statistics for NH_3 concentrations (μg m^{-3}) during 3 April 2014–2 April 2015 are shown in Table 1. Using a variety of chemical, physical and optical techniques, numerous studies have examined ambient NH_3 concentrations over the last three decades; however, few of them

ACPD
15, 34719–34763, 2015

were conducted in urban areas. As a comparison, we compiled previous work related to the measurement of urban NH_3 concentrations in Table 2.

The one year dataset (n = 8447; data availability 96.4 %) in the current study represents one of the longest on-line continuous measurement series of atmospheric NH_3 in China. During the study period, the NH_3 concentrations varied between 0.03 and 39.2 $\mu g\,m^{-3}$, with an average ($\pm 1\sigma$) of $5.5 \pm 3.9\,\mu g\,m^{-3}$. Domestically, the annual average NH_3 concentrations in Beijing and Xi'an were much higher than in Shanghai (see Table 2). This might be expected since Beijing and Xi'an are located in the North China Plain (NCP) and the Guanzhong Plain (GZP), respectively, two of the most intensive agricultural production regions in China. Moreover, the NH_3 loss from soil increases with an increase in soil pH value (Ju et al., 2009). Shanghai and its surrounding regions are dominated by the acid soils of paddy fields (Fig. 1) (Zhao et al., 2009), while Beijing and Xi'an are dominated by the alkaline soils of dry land (Wei et al., 2013). Internationally, the NH_3 concencentration level in Shanghai was similar to observations from cities in developed and middle-income countries, but much lower than those cities in emerging countries. This is particularly true when comparing with cities in South Asia (e.g., Delhi in India and Lahore in Pakistan), where there is a lack of basic sanitation facilities (e.g., public flush toilets) and significant animal populations (such as cow) coexist with people in urban areas. The higher NH_3 concentrations measured at surface sites in South Asia are consistent with spatial patterns from recent satellite remote sensing observations (Clarisse et al., 2009; Van Damme et al., 2014).

The variations of NH_3 in spring and summer were generally consistent with fluctuations of temperature (Fig. 2a). Monthly, from March to September, the NH_3 concentration first increased steadily, with the highest value in July, then decreased gradually, along with falling temperature (Fig. 2c). In summer (June to August), high temperatures favor NH_3 volatilization from urea and other N fertilizers applied to croplands (Fu et al., 2013; Huang et al., 2011; Ianniello et al., 2010; Meng et al., 2011). High temperatures in summer also favor NH_3 emission from other sources, such as animal housing, landfills, laystalls and pit latrines, animal manure, natural and fertilized soils, vegetation, and

ACPD
15, 34719–34763, 2015

municipal solid waste (Fu et al., 2013; Huang et al., 2011). Moreover, given that the equilibrium between ammonium nitrate particles and gaseous ammonia and nitric acid favors the gas phase compounds at higher temperature, warmer summer conditions promote dissociation of ammonium nitrate particles, shifting the ammonium/ammonia partitioning toward the gas phase (Behera et al., 2013). In this study, the average NH_3 concentration in summer ($7.3 \pm 4.9\,\mu g\,m^{-3}$; $n = 2181$) was $2.4\,\mu g\,m^{-3}$ or 41 % higher than the average of other seasons. The gap between summer and winter in Shanghai was similar to New York, but generally much lower than many other cities. Taking Beijing for example, according to Ianniello et al. (2010), the NH_3 concentration in summer was 460 % higher than in winter; this figure was 320 % in Xi'an between 2006 and 2007 (Cao et al., 2009). Smaller seasonal temperature differences and less agricultural activity in Shanghai could be the contributing factors.

Based on the "bottom-up" methodologies, previous emission inventories indicate that livestock feeding and N-fertilizer application contribute around 50 (48–54.9 %) and 35 % (33.4–40 %) of the total NH_3 emissions in the Yangtze River delta region (YRD for short, including Shanghai as well as 24 cities in the provinces of Jiangsu and Zhejiang), respectively (Fu et al., 2013; Huang et al., 2011, 2012). Agricultural production is also the dominant source of NH_3 emissions in most other regions worldwide (Bouwman et al., 1997; Olivier et al., 1998; Reis et al., 2009). However, performed at an urban level, many studies in Table 2 concluded that the concentrations and evolution of ambient NH_3 in urban areas were influenced by traffic emissions. As one of the world's largest megacities, Shanghai might expect contributions of vehicle-emitted NH_3 as well. NH_3 concentrations in the atmosphere, however, are also sensitive to other important factors such as changes in temperature, wind speed or direction, and boundary layer depth; other influential factors might include local or regional NH_3 emissions, dry and wet deposition, and gas-to-particle partitioning. The relative importance of such factors in controlling ambient NH_3 concentration may vary seasonally. For example, the highest and lowest daily NH_3 concentrations in Shanghai were observed on 10–11 July 2014 ($23.4 \pm 6.7\,\mu g\,m^{-3}$) and 10–11 March 2015 ($0.5 \pm 0.4\,\mu g\,m^{-3}$), respectively.

ACPD
15, 34719–34763, 2015

For the two periods, there was no significant difference between them in terms of wind speed and planetary boundary layer height (the relative humidity data in March period was missed). Although 19.6 mm of rainfall in the July period would be expected to lower NH_3 levels, the temperature on this high concentration date (28.4 °C) was much higher than on the low concentration March date (4.7 °C). Over a longer time frame, even though rainfall in summer was around twice the amount of rainfall in other seasons, other factors such as greater NH_3 emissions at higher temperature outweigh the wet scavenging effects of rainfall yielding higher summertime NH_3 concentrations. High NH_3 concentration episodes during burning of agricultural wheat residues, indicated by a strong and synchronous rise of trace aerosols from biomass burning (e.g., K^+ and BC), were also evident in late spring (Fig. 2b). The evolution of this pollution episode induced by biomass burning and its influence of on the air quality of Shanghai has been examined in our recent paper (Zou et al., 2015).

3.2 Effects of meteorological parameters

In the following, we will examine the (synergistic) effects of various meteorological parameters on measured NH_3 concentrations in Shanghai, because these factors may mask the effect of emissions on the measured NH_3 concentrations. Summary statistics for meteorological parameters during 3 April 2014–2 April 2015 are shown in Table 3.

Planetary boundary layer (PBL) height plays a vital role in determining the vertical dispersion of air pollutants that are emitted from the Earth surface. Decreasing height of PBL can normally hold the pollutants within the shallow surface layer so as to suppress the vertical atmospheric dilution. In many previous studies, as described above, the NH_3 concentrations in winter were much lower than those in summer. However, the NH_3 concentrations observed here in Shanghai during winter are relatively high. One may argue that weaker vertical mixing and shallow PBL layers in winter could trap NH_3 and contribute to elevated concentrations. In Fig. 3a, although the simulated average PBL height in winter is the lowest during our study period, there is no significant difference among different seasons. In Fig. 3b, the average PBL height in winter is even higher

ACPD
15, 34719–34763, 2015

than that in spring and summer. Therefore, a relatively high NH_3 concentration in winter at PD cannot be fully explained by the strength of vertical mixing or PBL height in this study.

Figure 4a suggests that temperature (T) is an important driver of the increase of NH_3 concentration in spring. No clear relationship is seen for other seasons. As the transitional period between winter and summer, springtime in Shanghai has the highest standard deviation of temperature during our study period (Table 3). Additionally, spring is known as the sowing season in South China, with the greatest application of N-containing fertilizers (mainly in the form of urea) of the year. Warming temperature tends to increase the rate of urea hydrolysis and ammonium conversion to NH_3, and therefore volatilization. For example, an increase in temperature from 7.2 to 15.6 °C can double volatilization loss when moisture content is kept the same (Ernst and Massey, 1960). For relative humidity (RH), there is no clear evidence to suggest RH as an important factor controlling the dynamics of NH_3 concentrations in any of the seasons (Fig. 4b). Figure S2 in the Supplement shows the RH and T dependent distributions of NH_3 concentration for each season. Given the generally poor relationship between the NH_3 concentration and T and RH as discussed above, NH_3 concentrations have no clear dependence on T and RH seasonally.

In Fig. 5a and b the distribution of hourly average wind speeds was calculated for values between 0 and 4.0 $m\,s^{-1}$ (99.5 % of occurrence). Figure 5a shows that there is a highly significant relationship between WS and NH_3 concentration ($R^2 = 0.91$, $p < 0.001$). The highest average NH_3 concentrations were measured under the lowest wind speeds and the lowest concentrations were measured at the highest wind speeds. There is no clear relationship between wind frequency (the number of wind occurrence) and average NH_3 concentration or WS during the study period (Fig. 5c). Figure S3 in the Supplement shows WS/WD dependence of NH_3 concentrations in different seasons. The distribution of NH_3 concentration showed an obvious concentration gradient as a function of WS. Seasonally, there are different preferential wind directions for the highest NH_3 concentration values. Generally, an overwhelming higher T

ACPD
15, 34719–34763, 2015

in summer tends to greatly enhance the contribution of temperature-dependent emissions to the urban NH_3 budget from agricultural areas. And the nearby rural areas around Pudong supersite are in the direction of Southeast (Nanhui) and Northeast (Chongming) (Fig. 6d). However, it is unexpected that in Shanghai, almost all high NH_3 concentration values in summer are concentrated in the direction of South-Southwest-West (Supplement Fig. S3b), which strongly indicates that the urban area is one of the most important NH_3 emission regions in Shanghai.

Figure 6a and b shows the RH and T dependent distributions of NH_3 and WS for the entire study period, respectively. Although the distribution of higher NH_3 favors the condition of high $T (> 25\,^{\circ}C)$, low RH (< 60 %) and low WS ($< 1.2\,m\,s^{-1}$), Fig. 6a shows that there is no obvious concentration gradient as a function of RH and T (Note that in Supplement Fig. S2d, higher NH_3 concentrations in winter tend to occur at higher T for a given RH range of 60 to 80 %). This can be explained by the dominance of low WS (often lower than $1.2\,m\,s^{-1}$) during east-southeast and west-northwest wind directions associated with intense local sources for NH_3 within the city (Fig. 6c). In brief, our results suggest that there are some temperature-independent and important NH_3 sources in the urban area of Shanghai.

3.3 NH_3 diurnal profiles and insight into sources

Hourly observations over long-term periods offer a unique opportunity to provide robust diurnal profiles for each season. Figure 7 shows the average diurnal profiles of NH_3 and CO concentrations across seasons. Historically, CO emissions in Shanghai and its surrounding YRD region mainly came from iron and steel manufacturing and on-road vehicles, which contributed 34 and 30 % of the total, respectively in 2007 (Huang et al., 2011). Due to changing economic activity, emission sources of air pollutants in China are changing rapidly. For example, over the past several years, China has implemented a portfolio of plans to phase out its old-fashioned and small steel mills, and raise standards for industrial pollutant emissions (Chang et al., 2012). In contrast, China continuously experienced double digit growth in terms of auto sales during the

ACPD
15, 34719–34763, 2015

same period, and became the world's largest automobile market since 2009 (Chang, 2014). Consequently, on-road traffic has overtaken industrial sources as the dominant source of CO emissions in Eastern China (Zhao et al., 2012). In Fig. 7, CO shows a well-marked bimodal diurnal profile, with maxima in the morning (starting at 05:00 local time) and the evening (starting at 16:00 LT), consistent with the variation of traffic flow in Shanghai (Liu et al., 2012). Therefore, CO variation can be utilized as a robust indicator of vehicle emissions. NH_3 also displays a clear bimodal profile during all four seasons, similar to the CO diurnal profile, suggesting a significant influence of on-road traffic (with daily commuting) on ambient NH_3 concentrations in the urban environment of Shanghai.

Interestingly however, NH_3 shows different degrees of positive relationship with CO as a function of season (Fig. 8b). Specifically, during summertime, NH_3 displays a significant relationship with CO ($R^2 = 0.48$, $p < 0.001$), while this positive relationship is not observed during the winter season, when heavy traffic volume also occurs. As discussed above, the seasonal variation of NH_3 concentration in Shanghai during our study period was quite flat. The seasonal average CO concentrations at PD were 0.71, 0.61, 0.58, and 1.1 ppmv in spring, summer, autumn, and winter, respectively. And the CO level in wintertime was higher than other seasons. Moreover, Fig. 8c suggests that for all seasons, the source region of NH_3 in Shanghai is local-dominated. However, the atmospheric lifetime of CO is much longer than that of NH_3 (typically several hours depending on meteorology) (Asman et al., 1998). PSCF analysis for CO in winter suggests important contributions from north of Shanghai (Fig. 8a), a region that does not appear as important as a NH_3 source (Fig. 8c). Consequently, elevated regional background levels of CO from long-range transport appear to yield a poorer relationship between NH_3 and CO in wintertime (Fig. 8b).

3.4 The emission and transport of vehicle-sourced NH_3

Table S1 in the Supplement summarizes statistics of the NH_3 concentrations ($\mu g\,m^{-3}$) measured at each sampling point in and out of the Handan tunnel, which have also

ACPD
15, 34719–34763, 2015

been visualized in Fig. 9b. As expected, the highest average NH_3 concentration occurred at the exit of the tunnel (T-d). Although NH_3 concentration varied temporally, throughout the two months of observations, a large spatial gradient in NH_3 concentration at near-road sites was present in every sampling event, suggesting that an intensive NH_3 source from on-road traffic (not meteorological parameters) is the leading factor in governing the variation of ambient NH_3 concentration in a road-side environment. The NH_3 concentrations in the tunnel were increased with distance from the entrance of the tunnel (T-a). The NH_3 concentration at T-d ($64.9 \pm 11.5\,\mu g\,m^{-3}$) was over 5 times that at T-a ($12.6 \pm 3.3\,\mu g\,m^{-3}$). Moreover, the lowest NH_3 concentration value obtained at T-d ($47.0\,\mu g\,m^{-3}$) was still nearly $10\,\mu g\,m^{-3}$ or 20 % higher than the highest value of other sites (Supplement Table S1). These observations provide compelling evidence that on-road traffic is an important emission source of NH_3 in the urban atmosphere. Given that there is a significant loss of vehicle exhaust from the tunnel through an array of ventilation orifices in the middle section of the tunnel, the NH_3 concentration at T-b ($29.2 \pm 6.6\,\mu g\,m^{-3}$) was close to that at T-c ($31.5 \pm 5.9\,\mu g\,m^{-3}$). If we taking into account of the Physical Distance (PD; 300 m) and the NH_3 Concentration Gap (CG; $33.4 \pm 11.5\,\mu g\,m^{-3}$) between T-c and T-d, the Cross Section of tunnel bore (CS; $70\,m^3$), the average Wind Speed (WS; $5\,m\,s^{-1}$) and Traffic Flow (TF; $120\,000\,vehicles\,day^{-1}$), we can obtain an approximate mileage-based NH_3 Emission Factor (EF) of $28 \pm 5\,mg\,km^{-1}$ for a single vehicle using the following equation:

$$EF = \frac{CG \times CS \times WS \times 86\,400}{TF \times PD} \quad (1)$$

where 86 400 is the number of seconds in a day. This NH_3 emission factor was similar to that observed for the Gurbrist tunnel in Switzerland ($31 \pm 4\,mg\,km^{-1}$) (Emmenegger et al., 2004) and the Caldecott tunnel in California ($49 \pm 3\,mg\,km^{-1}$) (Kean et al., 2000), while much lower than that recently measured in Guangzhou, China ($230 \pm 14\,mg\,km^{-1}$) (Liu et al., 2014). Based on the emission factor we developed, a population of 3.04 million vehicles (average mileage of $15\,000\,km\,yr^{-1}$) in Shanghai would produce around

ACPD
15, 34719–34763, 2015

1300 t NH_3 in 2014. This is very close to the "bottom-up" emission inventory in Shanghai for 2010 (1581.1 t) (Chang, 2014). Previous emission inventories in Shanghai (e.g., Huang et al., 2011 and Fu et al., 2012) made a significant underestimation of the NH_3 emissions from city areas. When compared with the NH_3 emissions from city area, the contribution of on-road traffic can reach 12 % of the total NH_3 emissions in Shanghai city areas (10 742 t) (Chang, 2014). Moreover, model results have shown that over half of agricultural NH_3 emissions would be deposited downwind of its source within 10 km depending on local meteorological conditions (Asman et al., 1998). Therefore, the relative contribution of NH_3 emissions from on-road traffic to urban PM pollution could be higher than the share of its mass contribution. Given that precisely estimating the EF of NH_3 from on-road traffic is beyond the scope of this paper, more research is needed to pinpoint this parameter in order to accurately quantify the amount of NH_3 emissions from vehicles.

From the tunnel exit to the open environment, the average NH_3 concentration at T-d ($64.9 \pm 11.5\,\mu g\,m^{-3}$) was 11 times more than that at $O_{310\,m}$ ($5.6 \pm 2.5\,\mu g\,m^{-3}$), and a general negative relationship was found between distance and ambient NH_3 concentration. Over the total measured distance, the maximum percent decrease was observed between the sites of T-d and $O_{0\,m}$ (50 m apart), indicating a rapid dispersion of vehicle-emitted NH_3 from the road tunnel. Still, Fig. 9c clearly shows that 64 % (48 %) of the NH_3 concentration we observed at the site of $O_{0\,m}$ ($O_{20\,m}$) can be explained by the simultaneous measurements of NH_3 concentration at T-d. No significant decrease in the gradients of NH_3 concentration was observed between the sites of $O_{150\,m}$ ($5.9 \pm 2.5\,\mu g\,m^{-3}$; $n = 6$) and $O_{310\,m}$ ($5.6 \pm 2.5\,\mu g\,m^{-3}$; $n = 6$), suggesting that the strongest impact of NH_3 emission and transport from local traffic flow on ambient NH_3 concentrations in the Shanghai urban area lies within 150 m distance.

ACPD
15, 34719–34763, 2015

4 Conclusions and outlook

This study linked a long-term and near real-time measurement of NH_3 at one of China's flagship supersites with a vehicle source-specific campaign performed in and out of a major freeway tunnel in Shanghai. The conclusions are shown as below:

- The average NH_3 concentration (mean $\pm 1\sigma$) between April 2014 and April 2015 was $5.5 \pm 3.9\,\mu g\,m^{-3}$. Seasonal NH_3 concentration levels varied in the following sequence: summer ($7.3 \pm 4.9\,\mu g\,m^{-3}$) > spring ($5.1 \pm 3.8\,\mu g\ m^{-3}$) ≈ winter ($5.0 \pm 3.4\,\mu g\,m^{-3}$) > fall ($4.5 \pm 2.3\,\mu g\,m^{-3}$).

- During spring, ambient NH_3 concentrations appeared to be influenced to some extent by temperature-dependent emissions, likely from agricultural activities including crop fertilization. No such relationship was apparent during other seasons. Measured NH_3 concentrations were highly dependent on wind speed, while mixing height of planetary boundary layer and relative humidity were not the main factors influencing seasonal NH_3 concentrations.

- The diurnal profile of NH_3 concentrations showed a typical bimodal cycle during four seasons, with maxima in the morning and the evening rush hours, suggesting a persistent influence of on-road traffic (with daily commuting) on ambient NH_3 levels in Shanghai.

- The NH_3 concentration in the exit of the Handan tunnel ($64.9 \pm 11.5\,\mu g\,m^{-3}$) was over 5 and 11 times higher than that in the tunnel entrance ($12.6 \pm 3.3\,\mu g\,m^{-3}$) and the ambient air ($5.6 \pm 2.5\,\mu g\,m^{-3}$), respectively, providing further compelling evidence that on-road traffic is an important NH_3 source. 1300 t vehicle-emitted NH_3 in 2014 was calculated based on a mileage-based NH_3 emission factor of $28 \pm 5\,mg\,km^{-1}$ we developed.

- A negative relationship was found between the distance and ambient NH_3 concentration in our near-road gradient experiment. Up to 64 % of ambient NH_3 con-

ACPD
15, 34719–34763, 2015

centration out of the tunnel can be explained by the vehicle-emitted NH_3 from the tunnel.

Unlike NH_3 emissions in agricultural areas, the NH_3 emissions in urban areas originate from a variety of stationary sources (industrial coal/oil/gas combustion, wastewater, landfill, compost and incineration), mobile sources and area sources (e.g., humans, green land, domestic fuel combustion). As a start, our study is far from fully elucidating the complex origins of urban NH_3 in Shanghai. Vehicle-emitted NH_3, while important, is likely not the only major source of NH_3. Additional useful investigative steps could include:

- Using isotopes as a source apportionment tool. Isotopic techniques have been proven to be useful tools for sources apportionment of gases and PM. Although the $\delta^{15}N$ values of NH_4^+ in rainwater and aerosols have been examined (Xiao et al., 2015; Xiao and Liu, 2002; Xiao et al., 2012), atmospheric NH_3 has received much less attention. According to Felix et al. (2013), NH_3 emitted from volatilized sources has relatively low $\delta^{15}N$ values, allowing them to be distinctly differentiated from NH_3 emitted from fuel-related sources (e.g., on-road traffic) that are characterized by relatively high $\delta^{15}N$ values.

- Using chemical transport modeling (CTM) as a cost-effective analysis tool. CTM has the potential to capture the complex atmospheric behavior of NH_3. Moreover, NH_3 emission reduction targets are represented as constraints in the optimization problem, and have a major influence on overall costs of a cost-effective solution and their distribution across different sources and economic sectors. Through sensitivity analyses of specific emission source or assuming possible emission control scenarios, CTM can contribute to the setting of effective emission reduction strategies to achieve cost-effective improvements in air quality.

The Supplement related to this article is available online at doi:10.5194/acpd-15-34719-2015-supplement.

ACPD
15, 34719–34763, 2015

Acknowledgements. Special thanks go to Tony Dore (CEH, UK), Yunting Fang (CAS, CN) and Fujiang Wang (Fudan, CN) for their insightful comments. This work was supported financially by the National Natural Science Foundation of China (Grant Nos. 21377029, 21277030 and 41405115). Yunhua Chang acknowledges the support of the Gao Tingyao scholarship and the Qingyue Environmental Data Center. The authors declare no competing financial interest.

References

Aneja, V. P., Chauhan, J. P., and Walker, J. T.: Characterization of atmospheric ammonia emissions from swine waste storage and treatment lagoons, J. Geophys. Res., 105, 11535–11545, doi:10.1029/2000JD900066, 2003.

Asman, W. A., Sutton, M. A., and Schjørring, J. K.: Ammonia: emission, atmospheric transport and deposition, New Phytol., 139, 27–48, doi:10.1046/j.1469-8137.1998.00180.x, 1998.

Bari, A., Ferraro, V., Wilson, L. R., Luttinger, D., and Husain, L.: Measurements of gaseous HONO, HNO_3, SO_2, HCl, NH_3, particulate sulfate and $PM_{2.5}$ in New York, NY, Atmos. Environ., 37, 2825–2835, doi:10.1016/S1352-2310(03)00199-7, 2003.

Behera, S. N., Sharma, M., Aneja, V. P., and Balasubramanian, R.: Ammonia in the atmosphere: a review on emission sources, atmospheric chemistry and deposition on terrestrial bodies, Environ. Sci. Pollut. R., 20, 8092–8131, doi:10.1007/s11356-013-2051-9, 2013.

Bettez, N. D., Marino, R., Howarth, R. W., and Davidson, E. A.: Roads as nitrogen deposition hot spots, Biogeochemistry, 114, 149–163, doi:10.1007/s10533-013-9847-z, 2013.

Bishop, G. A. and Stedman, D. H.: Reactive nitrogen species emission trends in three light-/medium-duty United States fleets, Environ. Sci. Technol., 49, 11234–11240, doi:10.1021/acs.est.5b02392, 2015.

Biswas, K. F., Ghauri, B. M., and Husain, L.: Gaseous and aerosol pollutants during fog and clear episodes in South Asian urban atmosphere, Atmos. Environ., 42, 7775–7785, doi:10.1016/j.atmosenv.2008.04.056, 2008.

Blanchard, C. L., Roth, P. M., Tanenbaum, S. J., Ziman, S. D., and Seinfeld, J. H.: The use of ambient measurements to identify which precursor species limit aerosol nitrate formation, JAPCA J. Air Waste MA, 50, 2073–2084, doi:10.1080/10473289.2000.10464239, 2000.

ACPD
15, 34719–34763, 2015

Bouwman, A. F., Lee, D. S., Asman, W. A. H., Dentener, F. J., Van Der Hoek, K. W., and Olivier, J. G. J.: A global high-resolution emission inventory for ammonia, Global Biogeochem. Cy., 11, 561–587, doi:10.1029/97GB02266, 1997.

Brito, J., Rizzo, L. V., Herckes, P., Vasconcellos, P. C., Caumo, S. E. S., Fornaro, A., Ynoue, R. Y., Artaxo, P., and Andrade, M. F.: Physical–chemical characterisation of the particulate matter inside two road tunnels in the São Paulo Metropolitan Area, Atmos. Chem. Phys., 13, 12199–12213, doi:10.5194/acp-13-12199-2013, 2013.

Brook, J. R., Wiebe, A. H., Woodhouse, S. A., Audette, C. V., Dann, T. F., Callaghan, S., Piechowski, M., Dabek-Zlotorzynska, E., and Dloughy, J. F.: Temporal and spatial relationships in fine particle strong acidity, sulphate, PM_{10}, and $PM_{2.5}$ across multiple Canadian locations, Atmos. Environ., 31, 4223–4236, doi:10.1016/S1352-2310(97)00248-3, 1997.

Broxton, P. D., Zeng, X., Sulla-Menashe, D., and Troch, P. A.: A global land cover climatology using MODIS data, J. Appl. Meteorol. Clim., 53, 1593–1605, doi:10.1175/JAMC-D-13-0270.1, 2014.

Cadle, S. H., Countess, R. J., and Kelly, N. A.: Nitric acid and ammonia in urban and rural locations, Atmos. Environ., 16, 2501–2506, doi:10.1016/0004-6981(82)90141-X, 1982.

Cao, J. J., Zhang, T., Chow, J. C., Watson, J. G., Wu, F., and Li, H.: Characterization of atmospheric ammonia over Xi'an, China, Aerosol Air Qual. Res., 9, 277–289, doi:10.4209/aaqr.2008.10.0043, 2009.

Cape, J. N., Tang, Y. S., Van Dijk, N., Love, L., Sutton, M. A., and Palmer, S. C. F.: Concentrations of ammonia and nitrogen dioxide at roadside verges, and their contribution to nitrogen deposition, Environ. Pollut., 132, 469–478, doi:10.1016/j.envpol.2004.05.009, 2004.

Chang, Y. H.: Non-agricultural ammonia emissions in urban China, Atmos. Chem. Phys. Discuss., 14, 8495–8531, doi:10.5194/acpd-14-8495-2014, 2014.

Chang, Y. H., Liu, X., Dore, A. J., and Li, K.: Stemming $PM_{2.5}$ pollution in China: re-evaluating the role of ammonia, aviation and non-exhaust road traffic emissions, Environ. Sci. Technol., 46, 13035–13036, doi:10.1021/es304806k, 2012.

Clarisse, L., Clerbaux, C., Dentener, F., Hurtmans, D., and Coheur, P. F.: Global ammonia distribution derived from infrared satellite observations, Nat. Geosci., 2, 479–483, doi:10.1038/ngeo551, 2009.

Draxler, R. R. and Rolph, G. D.: HYSPLIT (HYbrid Single-Particle Lagrangian Integrated Trajectory) Model access via NOAA ARL READY Website, Rep., NOAA Air Resources Laboratory,

ACPD
15, 34719–34763, 2015

Silver Spring, MD, USA, available at: http://ready.arl.noaa.gov/HYSPLIT.php (last access: 15 October 2015), 1997.
Durbin, T. D., Wilson, R. D., Norbeck, J. M., Miller, J. W., Huai, T., and Rhee, S. H.: Estimates of the emission rates of ammonia from light-duty vehicles using standard chassis dynamometer test cycles, Atmos. Environ., 36, 1475–1482, doi:10.1016/S1352-2310(01)00583-0, 2002.
Emmenegger, L., Mohn, J., Sigrist, M., Marinov, D., Steinemann, U., Zumsteg, F., and Meier, M.: Measurement of ammonia emissions using various techniques in a comparative tunnel study, Int. J. Environ. Pollut., 22, 326–341, doi:10.1504/IJEP.2004.005547, 2004.
Ernst, J. W. and Massey, H. F.: The effects of several factors on volatilization of ammonia formed from urea in the soil, Soil Sci. Soc. Am. Pro., 24, 87–90, doi:10.2136/sssaj1960.03615995002400020007x, 1960.
Felix, J. D., Elliott, E. M., Gish, T. J., McConnell, L. L., and Shaw, S. L.: Characterizing the isotopic composition of atmospheric ammonia emission sources using passive samplers and a combined oxidation-bacterial denitrifier approach, Rapid Commun. Mass Sp., 27, 2239–2246, doi:10.1002/rcm.6679, 2013.
Felix, J. D., Elliott, E. M., Gish, T. J., Maghirang, R., Cambal, L., and Clougherty, J.: Examining the transport of ammonia emissions across landscapes using nitrogen isotope ratios, Atmos. Environ., 95, 563–570, doi:10.1016/j.atmosenv.2014.06.061, 2014.
Fountoukis, C., Nenes, A., Sullivan, A., Weber, R., Van Reken, T., Fischer, M., Matías, E., Moya, M., Farmer, D., and Cohen, R. C.: Thermodynamic characterization of Mexico City aerosol during MILAGRO 2006, Atmos. Chem. Phys., 9, 2141–2156, doi:10.5194/acp-9-2141-2009, 2009.
Fraser, M. P. and Cass, G. R.: Detection of excess ammonia emissions from in-use vehicles and the implications for fine particle control, Environ. Sci. Technol., 32, 1053–1057, doi:10.1021/es970382h, 1998.
Fu, X., Wang, S., Zhao, B., Xing, J., Cheng, Z., Liu, H., and Hao, J.: Emission inventory of primary pollutants and chemical speciation in 2010 for the Yangtze River Delta region, China, Atmos. Environ., 70, 39–50, doi:10.1016/j.atmosenv.2012.12.034, 2013.
Gay, S. W., Schmidt, D. R., Clanton, C. J., Janni, K. A., Jacobson, L. D., and Weisberg, S.: Odor, total reduced sulfur, and ammonia emissions from animal housing facilities and manure storage units in Minnesota, Appl. Eng. Agric., 19, 347–360, doi:10.13031/2013.13663, 2003.

ACPD
15, 34719–34763, 2015

Giroux, M., Esclassan, J., Arnaud, C., and Chalé, J. J.: Analysis of levels of nitrates and derivatives of ammonia in an urban atmosphere, Sci. Total Environ., 196, 247–254, doi:10.1016/S0048-9697(96)05423-X, 1997.

Gong, L., Lewicki, R., Griffin, R. J., Flynn, J. H., Lefer, B. L., and Tittel, F. K.: Atmospheric ammonia measurements in Houston, TX using an external-cavity quantum cascade laser-based sensor, Atmos. Chem. Phys., 11, 9721–9733, doi:10.5194/acp-11-9721-2011, 2011.

Gong, L., Lewicki, R., Griffin, R. J., Tittel, F. K., Lonsdale, C. R., Stevens, R. G., Pierce, J., Malloy, Q., Travis, S., Bobmanuel, L., Lefer, B., and Flynn, J. H.: Role of atmospheric ammonia in particulate matter formation in Houston during summertime, Atmos. Environ., 77, 893–900, doi:10.1016/j.atmosenv.2013.04.079, 2013.

Heald, C. L., Collett Jr., J. L., Lee, T., Benedict, K. B., Schwandner, F. M., Li, Y., Clarisse, L., Hurtmans, D. R., Van Damme, M., Clerbaux, C., Coheur, P.-F., Philip, S., Martin, R. V., and Pye, H. O. T.: Atmospheric ammonia and particulate inorganic nitrogen over the United States, Atmos. Chem. Phys., 12, 10295–10312, doi:10.5194/acp-12-10295-2012, 2012.

Heeb, N. V., Forss, A. M., Brühlmann, S., Lüscher, R., Saxer, C. J., and Hug, P.: Three-way catalyst-induced formation of ammonia-velocity-and acceleration-dependent emission factors, Atmos. Environ., 40, 5986–5997, doi:10.1016/j.atmosenv.2005.12.035, 2006.

Heeb, N. V., Saxer, C. J., Forss, A. M., and Brühlmann, S.: Trends of NO^-, NO_2^-, and NH_3-emissions from gasoline-fueled Euro-3-to Euro-4-passenger cars, Atmos. Environ., 42, 2543–2554, doi:10.1016/j.atmosenv.2007.12.008, 2008.

Huai, T., Durbin, T. D., Younglove, T., Scora, G., Barth, M., and Norbeck, J. M.: Vehicle specific power approach to estimating on-road NH_3 emissions from light-duty vehicles, Environ. Sci. Technol., 39, 9595–9600, doi:10.1021/es050120c, 2005.

Huang, C., Chen, C. H., Li, L., Cheng, Z., Wang, H. L., Huang, H. Y., Streets, D. G., Wang, Y. J., Zhang, G. F., and Chen, Y. R.: Emission inventory of anthropogenic air pollutants and VOC species in the Yangtze River Delta region, China, Atmos. Chem. Phys., 11, 4105–4120, doi:10.5194/acp-11-4105-2011, 2011.

Huang, K., Zhuang, G., Lin, Y., Fu, J. S., Wang, Q., Liu, T., Zhang, R., Jiang, Y., Deng, C., Fu, Q., Hsu, N. C., and Cao, B.: Typical types and formation mechanisms of haze in an Eastern Asia megacity, Shanghai, Atmos. Chem. Phys., 12, 105–124, doi:10.5194/acp-12-105-2012, 2012.

ACPD
15, 34719–34763, 2015

Huang, K., Fu, J. S., Hsu, N. C., Gao, Y., Dong, X., Tsay, S. C., and Lam, Y. F.: Impact assessment of biomass burning on air quality in Southeast and East Asia during BASE-ASIA, Atmos. Environ., 78, 291–302, doi:10.1016/j.atmosenv.2012.03.048, 2013a.

Huang, K., Zhuang, G., Lin, Y., Wang, Q., Fu, J. S., Fu, Q., Liu, T., and Deng, C.: How to improve the air quality over megacities in China: pollution characterization and source analysis in Shanghai before, during, and after the 2010 World Expo, Atmos. Chem. Phys., 13, 5927–5942, doi:10.5194/acp-13-5927-2013, 2013b.

Huang, R. J., Zhang, Y., Bozzetti, C., Ho, K. F., Cao, J. J., Han, Y., Daellenbach, K., Slowik, J., Platt, S., Canonaco, F., Zotter, P., Wolf, R., Pieber, S., Bruns, E., Crippa, M., Ciarelli, G., Piazzalunga, A., Schwilowski, M., Abbaszade, G., Schnelle-Kreis, J., Zimmermann, R., An, Z., Szidat, S., Baltensperger, U., El Haddad, L., and Prévôt, A. S.: High secondary aerosol contribution to particulate pollution during haze events in China, Nature, 514, 218–222, doi:10.1038/nature13774, 2014.

Ianniello, A., Spataro, F., Esposito, G., Allegrini, I., Rantica, E., Ancora, M. P., Hu, M., and Zhu, T.: Occurrence of gas phase ammonia in the area of Beijing (China), Atmos. Chem. Phys., 10, 9487–9503, doi:10.5194/acp-10-9487-2010, 2010.

Ju, X. T., Xing, G. X., Chen, X. P., Zhang, S. L., Zhang, L. J., Liu, X. J., Cui, Z. L., Yin, B., Christie, P., Zhu, Z. L., and Zhang, F. S.: Reducing environmental risk by improving N management in intensive Chinese agricultural systems, P. Natl. Acad. Sci. USA, 106, 3041–3046, doi:10.1073/pnas.0813417106, 2009.

Kawashima, S. and Yonemura, S.: Measuring ammonia concentration over a grassland near livestock facilities using a semiconductor ammonia sensor, Atmos. Environ., 35, 3831–3839, doi:10.1016/S1352-2310(01)00145-5, 2001.

Kean, A. J., Harley, R. A., Littlejohn, D., and Kendall, G. R.: On-road measurement of ammonia and other motor vehicle exhaust emissions, Environ. Sci. Technol., 34, 3535–3539, doi:10.1021/es991451q, 2000.

Kean, A. J., Littlejohn, D., Ban-Weiss, G. A., Harley, R. A., Kirchstetter, T. W., and Lunden, M. M.: Trends in on-road vehicle emissions of ammonia, Atmos. Environ., 43, 1565–1570, doi:10.1016/j.atmosenv.2008.09.085, 2009.

Lamarque, J.-F., Bond, T. C., Eyring, V., Granier, C., Heil, A., Klimont, Z., Lee, D., Liousse, C., Mieville, A., Owen, B., Schultz, M. G., Shindell, D., Smith, S. J., Stehfest, E., Van Aardenne, J., Cooper, O. R., Kainuma, M., Mahowald, N., McConnell, J. R., Naik, V., Riahi, K., and van Vuuren, D. P.: Historical (1850–2000) gridded anthropogenic and biomass burn-

ACPD
15, 34719–34763, 2015

ing emissions of reactive gases and aerosols: methodology and application, Atmos. Chem. Phys., 10, 7017–7039, doi:10.5194/acp-10-7017-2010, 2010.
Leaderer, B. P., Naeher, L., Jankun, T., Balenger, K., Holford, T. R., Toth, C., Sullivan, J., Wolfson, J. M., and Koutrakis, P.: Indoor, outdoor, and regional summer and winter concentrations of PM_{10}, $PM_{2.5}$, SO_4^{2-}, H^+, NH_4^+, NO_3^-, NH_3, and nitrous acid in homes with and without kerosene space heaters, Environ. Health Persp., 107, 223–231, doi:10.1289/ehp.99107223, 1999.
Lee, H. S., Wadden, R. A., and Scheff, P. A.: Measurement and evaluation of acid air pollutants in Chicago using an annular denuder system, Atmos. Environ., 27, 543–553, doi:10.1016/0960-1686(93)90211-G, 1993.
Lee, H. S., Kang, C. M., Kang, B. W., and Kim, H. K.: Seasonal variations of acidic air pollutants in Seoul, South Korea, Atmos. Environ., 33, 3143–3152, doi:10.1016/S1352-2310(98)00382-3, 1999.
Li, K., Liu, X., Song, W., Chang, Y., Hu, Y., and Tian, C.: Atmospheric nitrogen deposition at two sites in an arid environment of Central Asia, Plos One, 8, e67018, doi:10.1371/journal.pone.0067018, 2013.
Li, M.: Engineering design of the Handan Road tunnel in the Middle Ring Road, China Munic. Eng., 1, 34–38, 2007. (in Chinese with English abstract)
Li, Y. Q., Schwab, J. J., and Demerjian, K. L.: Measurements of ambient ammonia using a tunable diode laser absorption spectrometer: characteristics of ambient ammonia emissions in an urban area of New York City, J. Geophys. Res., 111, D10S02, doi:10.1029/2005JD006275, 2006.
Lin, J., Nielsen, C. P., Zhao, Y., Lei, Y., Liu, Y., and McElroy, M. B.: Recent changes in particulate air pollution over China observed from space and the ground: effectiveness of emission control, Environ. Sci. Technol., 44, 7771–7776, doi:10.1021/es101094t, 2010.
Lin, Y. C., Cheng, M. T., Ting, W. Y., and Yeh, C. R.: Characteristics of gaseous HNO_2, HNO_3, NH_3 and particulate ammonium nitrate in an urban city of Central Taiwan, Atmos. Environ., 40, 4725–4733, doi:10.1016/j.atmosenv.2006.04.037, 2006.
Liu, T., Wang, X., Wang, B., Ding, X., Deng, W., Lü, S., and Zhang, Y.: Emission factor of ammonia (NH_3) from on-road vehicles in China: tunnel tests in urban Guangzhou, Environ. Res. Lett., 9, 064027, doi:10.1088/1748-9326/9/6/064027, 2014.

ACPD
15, 34719–34763, 2015

Liu, Y., Wang, F. Xiao, Y., and Gao, S: Urban land uses and traffic "source-sink areas": evidence from GPS-enabled taxi data in Shanghai, Landscape Urban Plan., 106, 73–87, doi:10.1016/j.landurbplan.2012.02.012, 2012.

Livingston, C., Rieger, P., and Winer, A.: Ammonia emissions from a representative in-use fleet of light and medium-duty vehicles in the California South Coast Air Basin, Atmos. Environ., 43, 3326–3333, doi:10.1016/j.atmosenv.2009.04.009, 2009.

Ma, Z., Hu, X., Huang, L., Bi, J., and Liu, Y.: Estimating ground-level $PM_{2.5}$ in China using satellite remote sensing, Environ. Sci. Technol., 48, 7436–7444, doi:10.1021/es5009399, 2014.

Ma, Z., Hu, X., Sayer, A. M., Levy, R., Zhang, Q., Xue, Y., Tong, S., Bi, J., Huang, L., and Liu, Y.: Satellite-based spatiotemporal trends in $PM_{2.5}$ concentrations: China, 2004–2013, Environ. Health Persp., accepted, doi:10.1289/ehp.1409481, 2015.

Matsumoto, M. and Okita, T.: Long term measurements of atmospheric gaseous and aerosol species using an annular denuder system in Nara, Japan, Atmos. Environ., 32, 1419–1425, doi:10.1016/S1352-2310(97)00270-7, 1998.

McCurdy, T., Zelenka, M. P., Lawrence, P. M., Houston, R. M., and Burton, R.: Acid aerosols in the Pittsburgh Metropolitan area, Atmos. Environ., 33, 5133–5145, doi:10.1016/S1352-2310(99)00119-3, 1999.

Meng, Z. Y., Lin, W. L., Jiang, X. M., Yan, P., Wang, Y., Zhang, Y. M., Jia, X. F., and Yu, X. L.: Characteristics of atmospheric ammonia over Beijing, China, Atmos. Chem. Phys., 11, 6139–6151, doi:10.5194/acp-11-6139-2011, 2011.

Moeckli, M. A., Fierz, M., and Sigrist, M. W.: Emission factors for ethene and ammonia from a tunnel study with a photoacoustic trace gas detection system, Environ. Sci. Technol., 30, 2864–2867, doi:10.1021/es960152n, 1996.

Mount, G. H., Rumburg, B., Havig, J., Lamb, B., Westberg, H., Yonge, D., Johnson, K., and Kincaid, R.: Measurement of atmospheric ammonia at a dairy using differential optical absorption spectroscopy in the mid-ultraviolet, Atmos. Environ., 36, 1799–1810, doi:10.1016/S1352-2310(02)00158-9, 2002.

Nowak, J. B., Neuman, J. A., Bahreini, R., Brock, C. A., Middlebrook, A. M., Wollny, A. G., Holloway, J., Peischl, J., Ryerson, T., and Fehsenfeld, F. C.: Airborne observations of ammonia and ammonium nitrate formation over Houston, Texas, J. Geophys. Res., 115, D22304, doi:10.1029/2010JD014195, 2010.

ACPD
15, 34719–34763, 2015

Olivier, J. G. J., Bouwman, A. F., Van der Hoek, K. W., and Berdowski, J. J. M.: Global air emission inventories for anthropogenic sources of NO_x, NH_3 and N_2O in 1990, Environ. Pollut., 102, 135–148, doi:10.1016/S0269-7491(98)80026-2, 1998.

Pandolfi, M., Amato, F., Reche, C., Alastuey, A., Otjes, R. P., Blom, M. J., and Querol, X.: Summer ammonia measurements in a densely populated Mediterranean city, Atmos. Chem. Phys., 12, 7557–7575, doi:10.5194/acp-12-7557-2012, 2012.

Parmar, R. S., Satsangi, G. S., Lakhani, A., Srivastava, S. S., and Prakash, S.: Simultaneous measurements of ammonia and nitric acid in ambient air at Agra (27°10′N and 78°05′E) (India), Atmos. Environ., 35, 5979–5988, doi:10.1016/S1352-2310(00)00394-0, 2001.

Perrino, C., Catrambone, M., Di Bucchianico, A. D. M., and Allegrini, I.: Gaseous ammonia in the urban area of Rome, Italy and its relationship with traffic emissions, Atmos. Environ., 36, 5385–5394, doi:10.1016/S1352-2310(02)00469-7, 2002.

Phan, N. T., Kim, K. H., Shon, Z. H., Jeon, E. C., Jung, K., and Kim, N. J.: Analysis of ammonia variation in the urban atmosphere, Atmos. Environ., 65, 177–185, doi:10.1016/j.atmosenv.2012.10.049, 2013.

Pierson, W. R. and Brachaczek, W. W.: Emissions of ammonia and amines from vehicles on the road, Environ. Sci. Technol., 17, 757–760, doi:10.1021/es00118a013, 1983.

Pierson, W. R., Gertler, A. W., Robinson, N. F., Sagebiel, J. C., Zielinska, B., Bishop, G. A., Stedman, D., Zweidinger, R., and Ray, W. D.: Real-world automotive emissions-summary of studies in the Fort McHenry and Tuscarora Mountain tunnels, Atmos. Environ., 30, 2233–2256, doi:10.1016/1352-2310(95)00276-6, 1996.

Pinder, R. W., Adams, P. J., and Pandis, S. N.: Ammonia emission controls as a cost-effective strategy for reducing atmospheric particulate matter in the eastern United States, Environ. Sci. Technol., 41, 380–386, doi:10.1021/es060379a, 2007.

Pio, C. A., Santos, I. M., Anacleto, T. D., Nunes, T. V., and Leal, R. M.: Particulate and gaseous air pollutant levels at the Portuguese west coast, Atmos. Environ., 25, 669–680, doi:10.1016/0960-1686(91)90065-F, 1991.

Polissar, A. V., Hopke, P. K., and Poirot, R. L.: Atmospheric aerosol over Vermont: chemical composition and sources, Environ. Sci. Technol., 35, 4604–4621, doi:10.1021/es0105865, 2001.

Pryor, S. C., Anlauf, K., Boudries, H., Hayden, K., Schiller, C. L., and Wiebe, A.: Spatial and temporal variability of high resolution reduced nitrogen concentrations in the Fraser Valley, Atmos. Environ., 38, 5825–5836, doi:10.1016/j.atmosenv.2003.12.045, 2004.

ACPD
15, 34719–34763, 2015

Reche, C., Viana, M., Pandolfi, M., Alastuey, A., Moreno, T., Amato, F., Ripoll, A., and Querol, X.: Urban NH_3 levels and sources in a Mediterranean environment, Atmos. Environ., 57, 153–164, doi:10.1016/j.atmosenv.2012.04.021, 2012.

Reche, C., Viana, M., Karanasiou, A., Cusack, M., Alastuey, A., Artiñano, B., Revuelta, M., López-Mahía, P., Blanco-Heras, G., Rodríguez, S., Sánchez de la Campa, A., Fernández-Camacho, R., González-Castanedo, Y., Mantilla, E., Tang, S., and Querol, X.: Urban NH_3 levels and sources in six major Spanish cities, Chemosphere, 119, 769–777, doi:10.1016/j.chemosphere.2014.07.097, 2015.

Reis, S., Pinder, R. W., Zhang, M., Lijie, G., and Sutton, M. A.: Reactive nitrogen in atmospheric emission inventories, Atmos. Chem. Phys., 9, 7657–7677, doi:10.5194/acp-9-7657-2009, 2009.

Rodhe, L., Stintzing, A. R., and Steineck, S.: Ammonia emissions after application of human urine to a clay soil for barley growth, Nutr. Cycl. Agroecosys., 68, 191–198, doi:10.1023/B:FRES.0000019046.10885.ee, 2004.

Salem, A. A., Soliman, A. A., and El-Haty, I. A.: Determination of nitrogen dioxide, sulfur dioxide, ozone, and ammonia in ambient air using the passive sampling method associated with ion chromatographic and potentiometric analyses, Air Qual. Atmos. Health, 2, 133–145, doi:10.1007/s11869-009-0040-4, 2009.

Sather, M. E., Mathew, J., Nguyen, N., Lay, J., Golod, G., Vet, R., Cotie, J. Hertel, T., Aaboe, E., Callison, R., Adam, J., Keese, D., Freise, J., Hathcoat, A., Sakizzie, B., King, M., Lee, C., Oliva, S., San Miguel, G., Crow, L., and Geasland, F.: Baseline ambient gaseous ammonia concentrations in the Four Corners area and eastern Oklahoma, USA, J. Environ. Monitor., 10, 1319–1325, doi:10.1039/B807984F, 2008.

Saylor, R. D., Edgerton, E. S., Hartsell, B. E., Baumann, K., and Hansen, D. A.: Continuous gaseous and total ammonia measurements from the southeastern aerosol research and characterization (SEARCH) study, Atmos. Environ., 44, 4994–5004, doi:10.1016/j.atmosenv.2010.07.055, 2010.

Schlesinger, W. H. and Hartley, A. E.: A global budget for atmospheric NH_3, Biogeochemistry, 15, 191–211, doi:10.1007/BF00002936, 1992.

Seinfeld, J. H. and Pandis, S. N.: Atmospheric Chemistry and Physics: From Air Pollution to Climate Change, Wiley, New York, USA, 1998.

ACPD
15, 34719–34763, 2015

Sharma, S., Pathak, H., Datta, A., Saxena, M., Saud, T., and Mandal, T.: Study on mixing ratio of atmospheric ammonia and other nitrogen components, Proc. Int. Acad. Ecol. Environ. Sci., 1, 26–35, 2011.

Shelef, M. and McCabe, R. W.: Twenty-five years after introduction of automotive catalysts: what next?, Catal. Today, 62, 35–50, doi:10.1016/S0920-5861(00)00407-7, 2000.

Shon, Z. H., Ghosh, S., Kim, K. H., Song, S. K., Jung, K., and Kim, N. J.: Analysis of water-soluble ions and their precursor gases over diurnal cycle, Atmos. Res., 132, 309–321, doi:10.1016/j.atmosres.2013.06.003, 2013.

Singh, S. and Kulshrestha, U. C.: Abundance and distribution of gaseous ammonia and particulate ammonium at Delhi, India, Biogeosciences, 9, 5023–5029, doi:10.5194/bg-9-5023-2012, 2012.

Singh, S. and Kulshrestha, U. C.: Rural vs. urban gaseous inorganic reactive nitrogen in the Indo-Gangetic plains (IGP) of India, Environ. Res. Lett., 9, 125004, doi:10.1088/1748-9326/9/12/125004, 2014.

Skamarock, W. C., Klemp, J. B., Dudhia, J., Gill, D. O., Barker, D. M., Duda, M. G., Huang, X., Wang, W., and Powers, J. G.: A description of the advanced research WRF version 3, NCAR Tech. Note, NCAR/TN-475+STR, 8 pp., Natl. Cent. for Atmos. Res., Boulder, Colo., USA, available at: http://opensky.ucar.edu/islandora/object/technotes:500 (last access: 12 November 2015), 2008.

Stanier, C., Singh, A., Adamski, W., Baek, J., Caughey, M., Carmichael, G., Edgerton, E., Kenski, D., Koerber, M., Oleson, J., Rohlf, T., Lee, S. R., Riemer, N., Shaw, S., Sousan, S., and Spak, S. N.: Overview of the LADCO winter nitrate study: hourly ammonia, nitric acid and $PM_{2.5}$ composition at an urban and rural site pair during $PM_{2.5}$ episodes in the US Great Lakes region, Atmos. Chem. Phys., 12, 11037–11056, doi:10.5194/acp-12-11037-2012, 2012.

Suarez-Bertoa, R., Zardini, A., and Astorga, C.: Ammonia exhaust emissions from spark ignition vehicles over the New European driving cycle, Atmos. Environ., 97, 43–53, doi:10.1016/j.atmosenv.2014.07.050, 2014.

Suarez-Bertoa, R., Zardini, A. A., Lilova, V., Meyer, D., Nakatani, S., Hibel, F., Ewers, J., Clairotte, M., Hill, L., and Astorga, C.: Intercomparison of real-time tailpipe ammonia measurements from vehicles tested over the new world-harmonized light-duty vehicle test cycle (WLTC), Environ. Sci. Pollut. R., 22, 7450–7460, doi:10.1007/s11356-015-4267-3, 2015.

ACPD
15, 34719–34763, 2015

Sun, K., Tao, L., Miller, D. J., Khan, M. A., and Zondlo, M. A.: On-road ammonia emissions characterized by mobile, open-path measurements, Environ. Sci. Technol., 48, 3943–3950, doi:10.1021/es4047704, 2014.

Sutton, M., Dragosits, U., Y. Tang, and Fowler, D.: Ammonia emissions from non-agricultural sources in the UK, Atmos. Environ., 34, 855–869, doi:10.1016/S1352-2310(99)00362-3, 2000.

Sutton, M. A., Erisman, J. W., Dentener, F., and Möller, D.: Ammonia in the environment: from ancient times to the present, Environ. Pollut., 156, 583–604, doi:10.1016/j.envpol.2008.03.013, 2008.

Tanner, P. A.: Vehicle-related ammonia emissions in Hong Kong, Environ. Chem. Lett., 7, 37–40, doi:10.1007/s10311-007-0131-0, 2009.

Toro, R. A., Canales, M., Flocchini, R. G., and Morales, R. G.: Urban atmospheric ammonia in Santiago city, Chile, Aerosol Air Qual. Res., 14, 33–44, doi:10.4209/aaqr.2012.07.0189, 2014.

Van Damme, M., Clarisse, L., Heald, C. L., Hurtmans, D., Ngadi, Y., Clerbaux, C., Dolman, A. J., Erisman, J. W., and Coheur, P. F.: Global distributions, time series and error characterization of atmospheric ammonia (NH_3) from IASI satellite observations, Atmos. Chem. Phys., 14, 2905–2922, doi:10.5194/acp-14-2905-2014, 2014.

Vogt, E., A. Held, and Klemm, O.: Sources and concentrations of gaseous and particulate reduced nitrogen in the city of Münster (Germany), Atmos. Environ., 39, 7393–7402, doi:10.1016/j.atmosenv.2005.09.012, 2005.

Walker, J. T., Whitall, D. R., Robarge, W., and Paerl, H. W.: Ambient ammonia and ammonium aerosol across a region of variable ammonia emission density, Atmos. Environ., 38, 1235–1246, doi:10.1016/j.atmosenv.2003.11.027, 2004.

Wang, J., Xie, P., Qin, M., Ling, L., Ye, C., Liu, J., and Liu, W.: Study on the measurement of ambient ammonia in urban area based on open-path DOAS technique, Spectrosc. Spect. Anal., 32, 476–480, doi:10.3964/j.issn.1000-0593(2012)02-0476-05, 2012.

Wang, S. X., Xing, J., Jang, C. R., Zhu, Y., Fu, J. S., and Hao, J. M.: Impact assessment of ammonia emissions on inorganic aerosols in East China using response surface modeling technique, Environ. Sci. Technol., 45, 9293–9300, doi:10.1021/es2022347, 2011.

Wang, S. X., Zhao, B., Cai, S. Y., Klimont, Z., Nielsen, C. P., Morikawa, T., Woo, J. H., Kim, Y., Fu, X., Xu, J. Y., Hao, J. M., and He, K. B.: Emission trends and mitigation options for air pol-

ACPD
15, 34719–34763, 2015

lutants in East Asia, Atmos. Chem. Phys., 14, 6571–6603, doi:10.5194/acp-14-6571-2014, 2014.
Wang, W., Wang, S., Xu, J., Zhou, R., Shi, C., and Zhou, B.: Gas-phase ammonia and PM ammonium in a busy traffic area of Nanjing, China, Environ. Sci. Pollut. R., 9, 1–12, doi:10.1007/s11356-015-5397-3, 2015.
Wang, Y., Zhang, Q. Q., He, K., Zhang, Q., and Chai, L.: Sulfate-nitrate-ammonium aerosols over China: response to 2000–2015 emission changes of sulfur dioxide, nitrogen oxides, and ammonia, Atmos. Chem. Phys., 13, 2635–2652, doi:10.5194/acp-13-2635-2013, 2013.
Wei, S., Dai, Y., Liu, B., Zhu, A., Duan, Q., Wu, L., Ji, D., Ye, A., Yuan, H., Zhang, Q., Chen, D., Chen, M., Chu, J., Dou, Y., Guo, J., Li, H., Li, J., Liang, L., Liang, X., Liu, H., Liu, S., Miao, C., and Zhang, Y.: A China data set of soil properties for land surface modeling, J. Adv. Model. Earth Sy., 5, 212–224, doi:10.1002/jame.20026, 2013.
Xiao, H. W., Xiao, H. Y., Long, A. M., and Wang, Y. L.: Who controls the monthly variations of NH_4^+ nitrogen isotope composition in precipitation?, Atmos. Environ., 54, 201–206, doi:10.1016/j.atmosenv.2012.02.035, 2012.
Xiao, H. W., Xie, L. H., Long, A. M., Ye, F., Pan, Y. P., Li, D. N., Long, Z. H., Chen, L., Xiao, H. Y., and Liu, C. Q.: Use of isotopic compositions of nitrate in TSP to identify sources and chemistry in South China Sea, Atmos. Environ., 109, 70–78, doi:10.1016/j.atmosenv.2015.03.006, 2015.
Xiao, H. Y. and Liu, C. Q.: Sources of nitrogen and sulfur in wet deposition at Guiyang, southwest China, Atmos. Environ., 36, 5121–5130, doi:10.1016/S1352-2310(02)00649-0, 2002.
Yamamoto, N., Nishiura, H., Honjo, T., Ishikawa, Y., and Suzuki, K.: A long-term study of atmospheric ammonia and particulate ammonium concentrations in Yokohama, Japan, Atmos. Environ., 29, 97–103, doi:10.1016/1352-2310(94)00226-B, 1995.
Yan, X., Akimoto, H., and Ohara, T.: Estimation of nitrous oxide, nitric oxide and ammonia emissions from croplands in East, Southeast and South Asia, Glob. Change Biol., 9, 1080–1096, doi:10.1046/j.1365-2486.2003.00649.x, 2003.
Yao, X., Hu, Q., Zhang, L., Evans, G. J., Godri, K. J., and Ng, A. C.: Is vehicular emission a significant contributor to ammonia in the urban atmosphere?, Atmos. Environ., 80, 499–506, doi:10.1016/j.atmosenv.2013.08.028, 2013.
Ye, X., Ma, Z., Zhang, J., Du, H., Chen, J., Chen, H., Chen, H., Yang, X., Gao, W., and Geng, F.: Important role of ammonia on haze formation in Shanghai, Environ. Res. Lett., 6, 024019, doi:10.1088/1748-9326/6/2/024019, 2011.

ACPD
15, 34719–34763, 2015

Zhao, X., Xie, Y., Xiong, Z., Yan, X., Xing, G., and Zhu, Z.: Nitrogen fate and environmental consequence in paddy soil under rice-wheat rotation in the Taihu lake region, China. Plant Soil, 319, 225–234, doi:10.1007/s11104-008-9865-0, 2009.

Zhao, Y., Nielsen, C. P., McElroy, M. B., Zhang, L., and Zhang, J.: CO emissions in China: uncertainties and implications of improved energy efficiency and emission control, Atmos. Environ., 49, 103–113, doi:10.1016/j.atmosenv.2011.12.015, 2012.

Zhao, Y., Zhang, J., and Nielsen, C. P.: The effects of recent control policies on trends in emissions of anthropogenic atmospheric pollutants and CO_2 in China, Atmos. Chem. Phys., 13, 487–508, doi:10.5194/acp-13-487-2013, 2013.

Zheng, J., Ma, Y., Chen, M., Zhang, Q., Wang, L., Khalizov, A. F., Yao, L., Wang, Z., Wang, X., and Chen, L.: Measurement of atmospheric amines and ammonia using the high resolution time-of-flight chemical ionization mass spectrometry, Atmos. Environ., 102, 249–259, doi:10.1016/j.atmosenv.2014.12.002, 2015.

Zou, Z., Shan, F., Cai, Y., Chang, Y. H., and Zhao, Q.: Evolution of biomass burning on urban air quality: a case study of spring 2014 in Shanghai, Environ. Monit. Forewarn., 4, 4–8, 2015. (in Chinese with English abstract)

ACPD
15, 34719–34763, 2015

Table 1. Summary statistics of the NH_3 concentrations ($\mu g\,m^{-3}$) measured in Shanghai during 3 April 2014–2 April 2015. P10 and P90 represent the 10th and 90th concentration percentile, respectively.

	N	Mean	SD	Minimum	P10	Medium	P90	Maximum
All	8447	5.5	3.9	0.03	2.0	4.6	10.2	39.2
Spring	2204	5.1	3.8	0.03	1.7	4.1	9.6	25.1
Summer	2181	7.3	4.9	0.65	2.6	6.3	12.7	39.2
Autumn	1949	4.5	2.3	0.57	2.3	3.9	7.2	19.7
Winter	2113	5.0	3.4	0.43	1.8	4.3	9.3	30.7

ACPD
15, 34719–34763, 2015

Table 2. Ambient NH_3 concentration measurements in the urban atmosphere of China and other countries/regions.

Location	Period	Methodology	Time resolution	Concentration (μm^{-3})	Reference
East Asia					
Shanghai, CN	Apr 2014–Apr 2015	MARGA online monitor	hourly	5.5 ± 3.9	This study
Beijing, CN	Feb 2008–Jul 2010	Ogawa passive sampler	weekly	14.2 ± 10.6 (2008), 18.1 ± 13.8 (2009)	Meng et al. (2011)
Beijing, CN	Jan–Feb 2007, 8	Annular diffusion denuder	daily	5.5 ± 3.8 (winter), 25.4 ± 6.9 (summer)	Ianniello et al. (2010)
Xi'an, CN	Apr 2006–Apr 2007	Ogawa passive sampler	weekly	12.9/6.4/20.3 (annual/winter/summer)	Cao et al. (2009)
Nanjing, CN	Aug–Sep 2012	HRToF-CIMS [a]	1 Hz	1.3 ± 1.8 (industrial area)	Zheng et al. (2015)
Nanjing, CN	Jul–Aug 2013	Portable NH_3 online detector	hourly	6.7 (near road)	Wang et al. (2015)
Guangzhou, CN	Nov 2010	OP-DOAS [b]	2.5 min	1.6	Wang et al. (2012)
Urumqi, CN	Sep 2009–Aug 2010	Radiello passive sampler	biweekly	6.5	Li et al. (2013)
Hongkong, CN	Oct 2003–May 2006	Ogawa passive sampler	weekly	0.7 (rooftop) −7.1 (near road)	Tanner (2009)
Taichung, TW	Jan–Dec 2002	Annular diffusion denuder	12 h	8.5 ± 3.0	Lin et al. (2006)
Yohokama, JP	Jan 1987–Dec 1991	Glass flask sampling	3 h	2.5 ± 1.4 (winter), 8.7 ± 3.1 (summer)	Yamamoto et al. (1995)
Nara, JP	Jun 1994–May 1995	Annular diffusion denuder	12 h	1.7 (winter), 1.6 (summer)	Matsumoto and Okita (1998)
Seoul, KP	Oct 1996–Sep 1997	Annular diffusion denuder	daily;	4.3/0.7/38.6 (annual/winter/summer)	Lee et al. (1999)
Seoul, KP	Jan–Dec 2010	MARGA online monitor	hourly	6.8 ± 3.3 (spring), 11.2 ± 3.9 (summer)	Shon et al. (2013)
Seoul, KP	Sep 2010–Aug 2011	MARGA online monitor	hourly	8.4 ± 3.3	Phan et al. (2013)
North America					
New York, US	Jan 1999–Jun 2000	Annular diffusion denuder	daily	5.0/4.1/6.1 (annual/winter/summer)	Bari et al. (2003)
New York, US	Jan–Feb 2004	TDLAS [c]	< 1 min	0.6 (winter)	Li et al. (2006)
Chicago, US	Apr 1990–Mar 1991	Annular diffusion denuder	12 h	1.6 ± 1.7	Lee et al. (1993)
Pittsburgh, US	Jul–Sep 1993	Annular diffusion denuder	daily	3.9 ± 4.4 (summer)	McCurdy et al. (1999)
Los Angeles, US	May 1988–Sep 1994	Annular diffusion denuder	12 h	8.3	Blanchard et al. (2000)
Sacramento, US	Oct 1988–Sep 1994	Annular diffusion denuder	12 h	9.5	Blanchard et al. (2000)
Santa Barbara, US	May 1988–Sep 1994	Annular diffusion denuder	12 h	2.7	Blanchard et al. (2000)
Farmington, US	Dec 2006–Dec 2007	Ogawa passive sampler	3 week	1.2 ± 0.4	Sather et al. (2008)
Clinton, US	Jan–Dec 2000	Annular diffusion denuder	12 h	2.6 (winter), 6.2 (summer)	Walker et al. (2004)
Kinston, US	Jan–Dec 2000	Annular diffusion denuder	12 h	0.5 (winter), 2.7 (summer)	Walker et al. (2004)
Morehead, US	Jan–Dec 2000	Annular diffusion denuder	12 h	0.3 (winter), 0.7 (summer)	Walker et al. (2004)
Houston, US	Aug 2010	Quantum laser spectrometer	10 min	2.3 ± 1.9 (summer)	Gong et al. (2011)
Commerce, US	Nov–Dec 1978	Customed passive sampler	two days	2.6 (winter)	Cadle et al. (1982)
Vinton, US	May–Sep 1995	Ogawa passive sampler	biweekly	1.3 ± 0.4 (summer)	Leaderer et al. (1999)
Mexico city, MX	Mar 2006	Quantum laser spectrometer	6 min	17.7 ± 11.0 (spring)	Fountoukis et al. (2009)
Hamilton,CA	1992–1994	Annular diffusion denuder	daily	4.3	Brook et al. (1997)

ACPD
15, 34719–34763, 2015

Table 2. Continued.

Location	Period	Methodology	Time resolution	Concentration (μm^{-3})	Reference
Europe					
Edinburgh, UK	Apr–May 2002	ALPHA passive sampler	bimonthly	4.8 (spring)	Cape et al. (2004)
Münster, DE	Mar–Jul 2004	AMANDA [d]	10 min	3.9 (spring-summer)	Vogt et al. (2005)
Toulouse, FR	Mar 1985–Mar 1986	Nylon filter pack method	daily	3.8 (near road) – 19.8 (residential)	Giroux et al. (1997)
Rome, IT	May 2001–Mar 2002	Annular diffusion denuder	30 min	17.2 ± 2.7 (near road)	Perrino et al. (2002)
Al-Ain, AE	Apr 2005–Apr 2006	Ogawa passive sampler	biweekly	9.7 ± 4.8	Salem et al. (2009)
Barcelona, ES	May–Sep 2011	AiRRmonia online analyzer	1 min	2.2 ± 1.0 (near road), 5.6 ± 2.1 (mixed)	Pandolfi et al. (2012)
Barcelona, ES	Jan, Jul 2010; Jan 2011	ALPHA passive sampler	biweekly	4.4 (winter), 9.5 (summer)	Reche et al. (2012)
Barcelona, ES	Jan, Jul 2010; Jan 2011	ALPHA passive sampler	biweekly	4.5 ± 2.1 (winter), 9.2 ± 6.6 (winter)	Reche et al. (2015)
Madrid, ES	Mar, Jul 2010; Jul 2011	ALPHA passive sampler	biweekly	2.3 ± 1.3 (winter), 2.6 ± 1.8 (summer)	Reche et al. (2015)
Valencia, ES	Feb–Mar, Jun 2010; Feb–Mar 2011	ALPHA passive sampler	biweekly	1.5 ± 0.9 (winter), 0.5 ± 0.4 (summer)	Reche et al. (2015)
Huelva, ES	May–Jun, Nov 2010; May–Jun 2011	ALPHA passive sampler	biweekly	2.8 ± 3.8 (winter), 1.2 ± 0.9 (summer)	Reche et al. (2015)
Aveiro, PT	Aug 1988–May 1989	Nylon filter pack method	daily	3.5 ± 1.9	Pio et al. (1991)
South America					
Santiago, CL	Apr–Jun 2008	Ogawa passive sampler	monthly	15.0 ± 3.8 (spring)	Toro et al. (2014)
Sourth Asia					
Lahore, PK	Dec 2005–Feb 2006	Annular diffusion denuder	12 h	50.1 ± 16.9	Biswas et al. (2008)
Dayalbagh, IN	Feb, Jun 1997; Feb 1998	Annular diffusion denuder	3 h	12.5 ± 2.2	Parmar et al. (2001)
Delhi, IN	Sep–Oct 2008; Sep–Oct 2009	Chemiluminescence analyzer	1 h	13.5 ± 2.5 (2008), 14.4 ± 3.7 (2009)	Sharma et al. (2011)
Delhi, IN	Apr 2010–Nov 2011	Glass flask sampling	5 h	35.0 ± 16.8	Singh and Kulshrestha (2012)
Delhi, IN	Oct 2012–Sep 2013	Glass flask sampling	8 h	40.7 ± 16.8	Singh and Kulshrestha (2014)

[a] High resolution time-of-flight chemical ionization mass spectrometry.
[b] Open-path differential optical absorption spectroscopy.
[c] Tunable diode laser absorption spectrometer.
[d] Horizontal continuous-flow wet denuder.

ACPD
15, 34719–34763, 2015

Table 3. The average of temperature (°C), relative humidity (%), accumulated rainfall (mm) and simulated planetary boundary layer (PBL) height (m) in Shanghai (mean ± 1σ) during 3 Apr 2014–2 Apr 2015.

	Temperature	Relative humidity	Accumulated rainfall	Simulated PBL height
All	17.1 ± 8.2	72.4 ± 16.1	1271.5	454.0 ± 309.2
Spring	16.1 ± 6.1	63.7 ± 19.5	298.3	448.8 ± 311.9
Summer	25.7 ± 3.4	78.4 ± 12.5	550.7	460.6 ± 293.2
Autumn	19.8 ± 4.4	76.5 ± 13.0	221.4	482.6 ± 321.6
Winter	6.7 ± 3.3	67.0 ± 15.6	192.1	428.0 ± 307.4

ACPD
15, 34719–34763, 2015

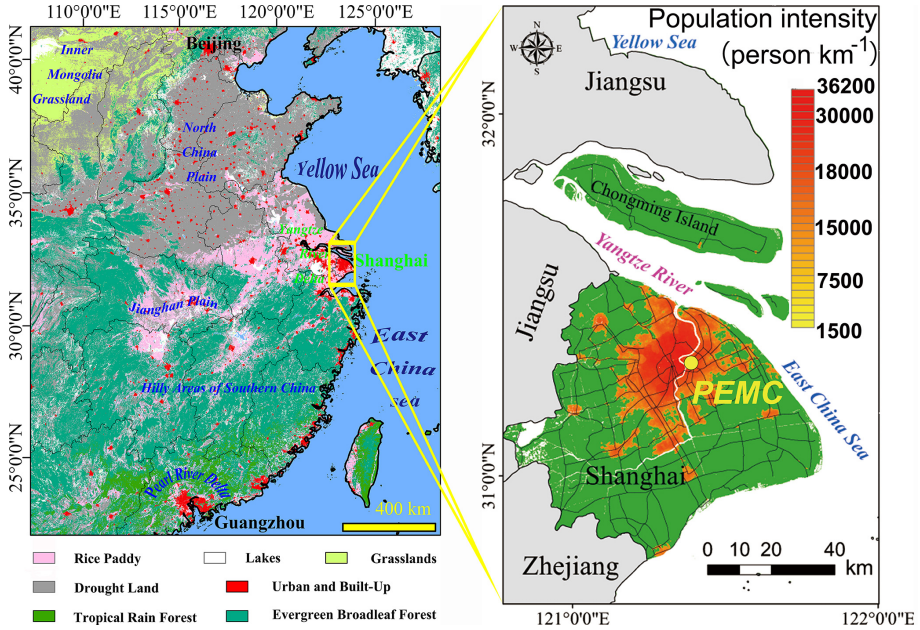

Figure 1. Location of the Pudong Environmental Monitoring Center (PEMC) supersite in Shanghai. The left panel shows various types of land use in eastern and southern China (adopted from, Broxton et al., 2014). The red areas and black lines in the right panel represent the urban areas and main roads in Shanghai, respectively.

ACPD
15, 34719–34763, 2015

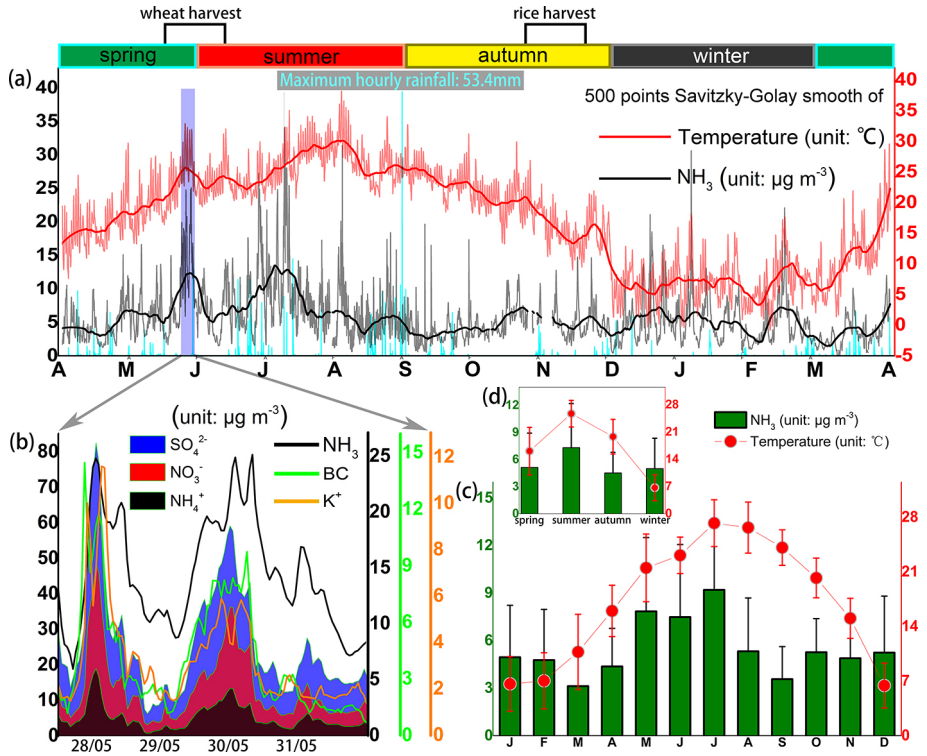

Figure 2. (a) Temporal variations of hourly NH_3 concentrations (gray) and temperature (red), along with 500-point Savitzky-Golay smoothed records in Shanghai from 3 April 2014 to 2 April 2015. Rainfall is shown in cyan. The vertical blue rectangle highlights NH_3 pollution episodes that occured during the wheat harvest season. **(b)** Time series of NH_3, BC, SO_4^{2-}, NO_3^-, NH_4^+, and K^+ concentrations during periods of pollution associated with biomass burning. Monthly **(c)** and seasonal **(d)** variations of NH_3 average concentrations and temperature.

ACPD
15, 34719–34763, 2015

The importance of vehicle emissions as a source of atmospheric ammonia

Y. H. Chang et al.

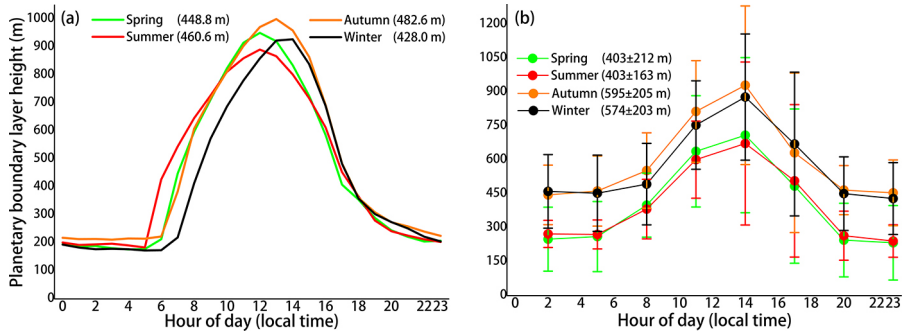

Figure 3. (a) Simulated diurnal profiles of the planetary boundary layer height in Shanghai during 3 April 2014–2 April 2015. **(b)** Daily evolution of the planetary boundary layer height (NOAA READY achieved GDAS data) in Shanghai from 12 April 2014 to 11 April 2015. The number in the legend represents the average planetary boundary layer height, by time of day, in different seasons.

ACPD
15, 34719–34763, 2015

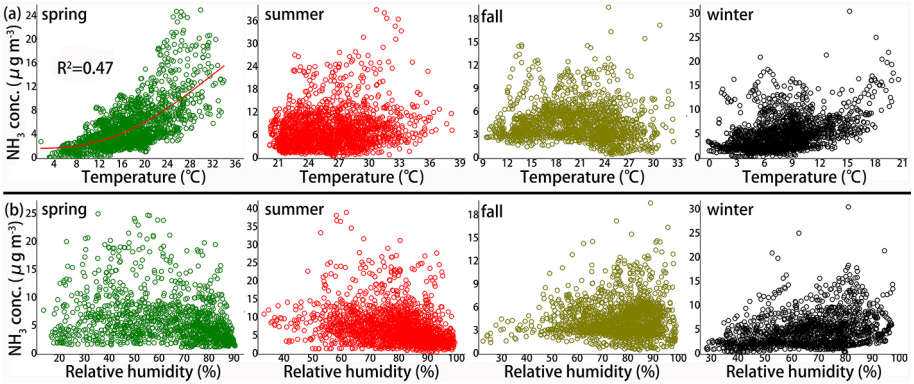

Figure 4. The relationship between hourly NH_3 concentration and hourly temperature **(a)** and hourly relative humidity **(b)** in four seasons at Pudong supersite between during 3 April 2014-2 April 2015.

ACPD
15, 34719–34763, 2015

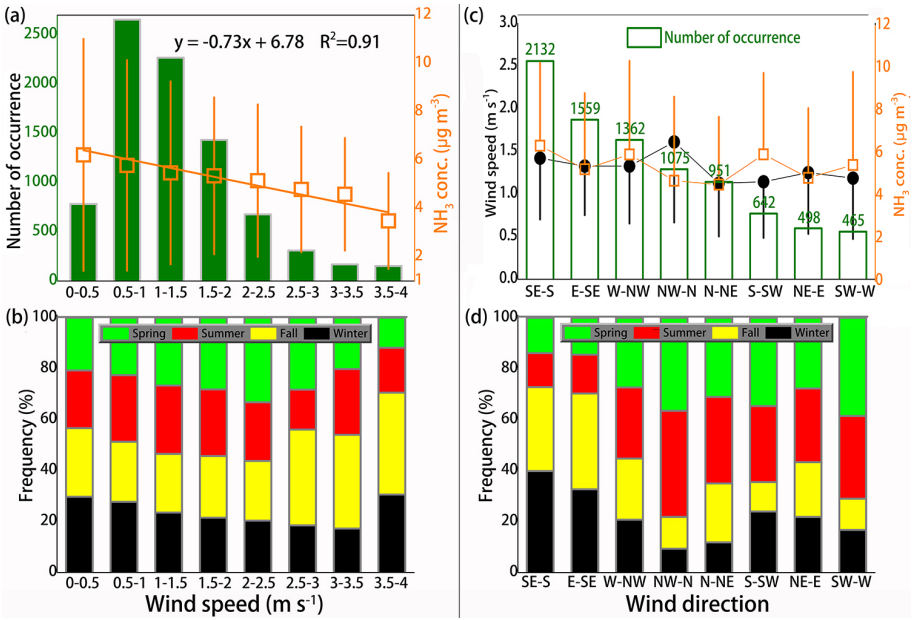

Figure 5. (a) Linear fitting of average NH_3 concentrations at different ranges of wind speed. The number of occurrences of wind (NOW) within each specific range of wind speed is shown as green columns. **(b)** Seasonal frequency distribution (%) of NOW at each specific range of wind speed. **(c)** The green boxes showing a descending order of the number of occurences of wind at different wind directions. The points in black and the squares in orange represent the average wind speed and NH_3 concentration for each specific wind direction, respectively. **(d)** Seasonal frequency distribution (%) of NOW at each specific wind direction.

ACPD
15, 34719–34763, 2015

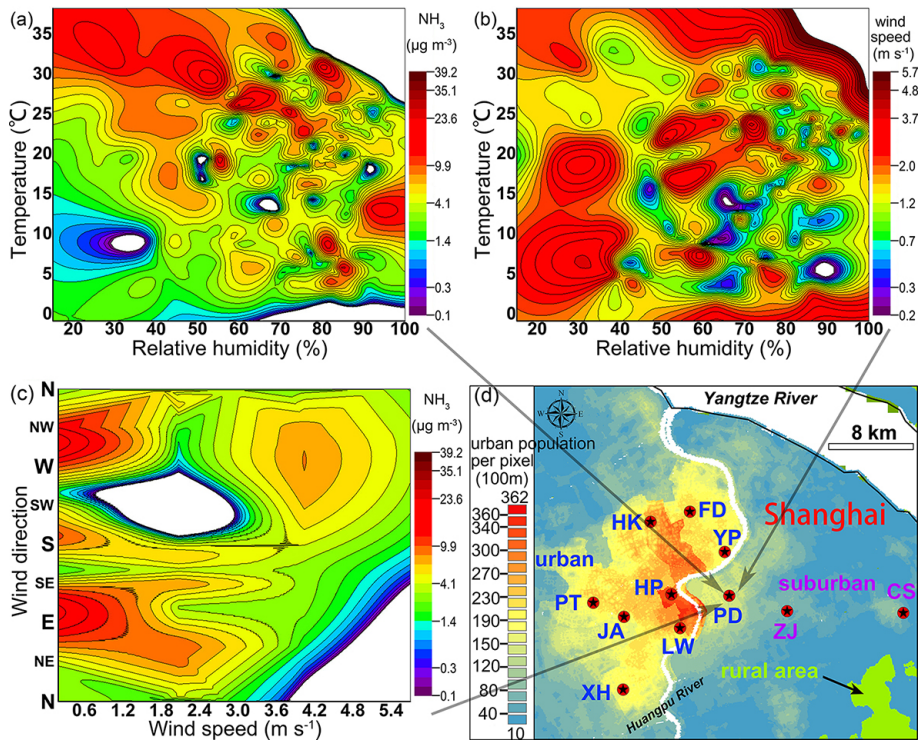

Figure 6. RH/T dependence of **(a)** NH_3 mass concentration and **(b)** WS, and **(c)** WS/WD dependence of NH_3 mass concentration at Pudong (PD) supersite for the year sampled. **(d)** The spatial distribution of environemtal monitoring network in Shanghai. FD represents Fudan university. The base map is the 2010 urban population density, derived from a newly released high-resolution (100 m × 100 m per pixel) population map of China (http://www.worldpop.org.uk/).

ACPD
15, 34719–34763, 2015

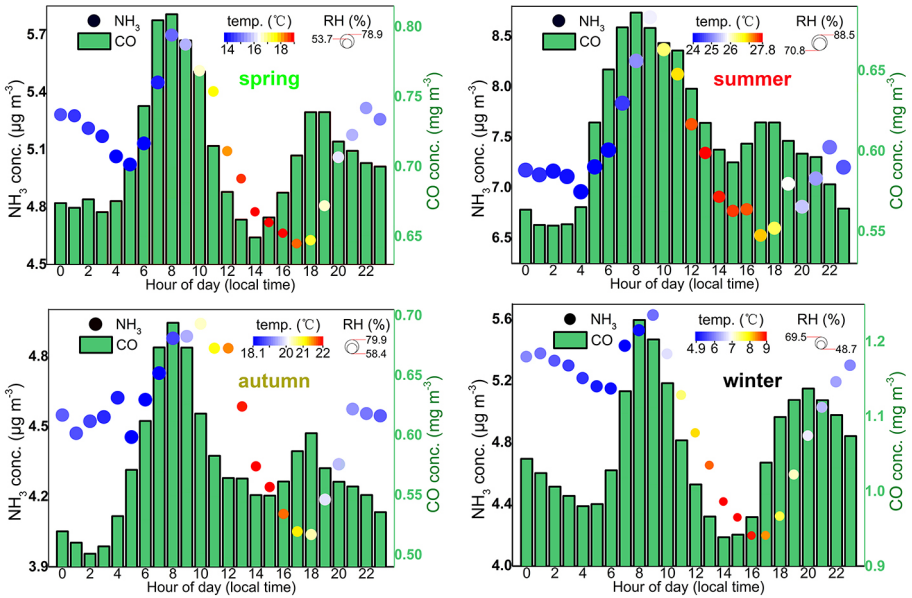

Figure 7. Seasonal diurnal profiles of NH_3 and CO concentrations in Shanghai. Color coded by hourly temperature and circle radius coded by hourly relative humidity.

ACPD
15, 34719–34763, 2015

The importance of vehicle emissions as a source of atmospheric ammonia

Y. H. Chang et al.

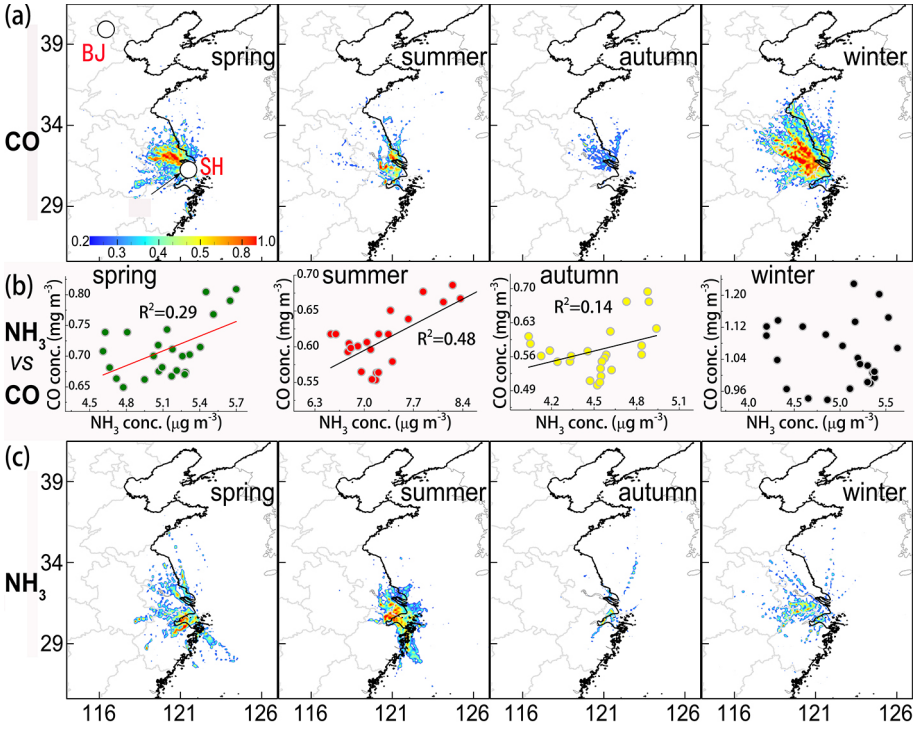

Figure 8. PSCF of CO **(a)** and NH_3 **(c)** during four seasons. The cities marked in each panel are Beijing (BJ) and Shanghai (SH). The color scales indicate the values of PSCF. **(b)** Relationship between hourly NH_3 and CO during four seasons.

ACPD
15, 34719–34763, 2015

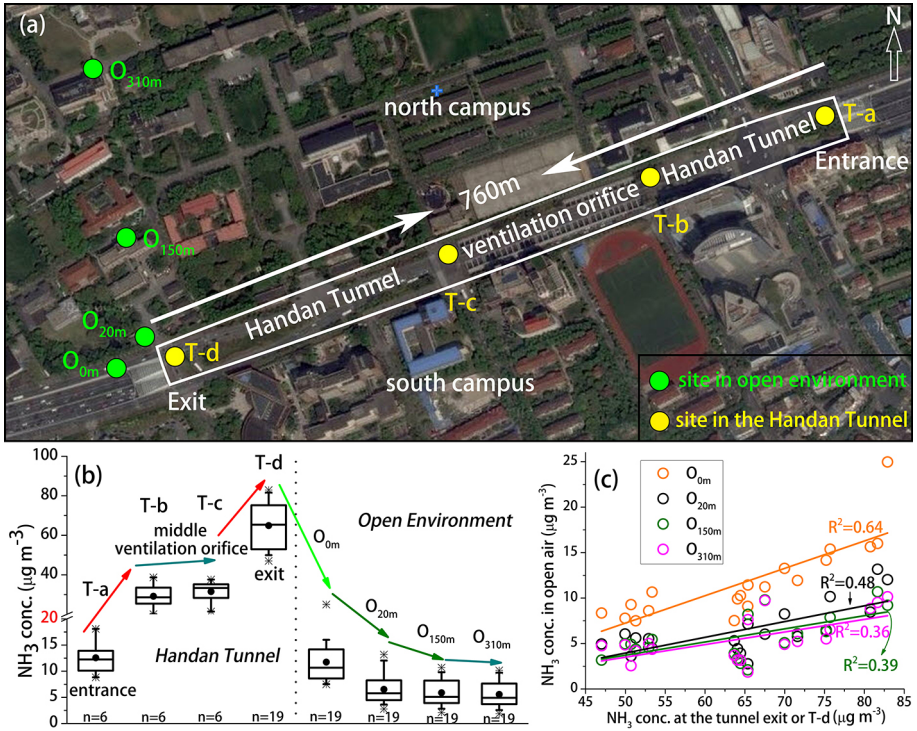

Figure 9. (a) Location of the eight sampling points in (labeled in yellow; inside the tunnel from the entrance to the exit) and out (labeled in green; varying in distance from the tunnel) of the Handan tunnel where atmospheric concentrations of NH_3 were measured using fritted glass bubblers. The campus of Fudan University was separated into north and south parts by the tunnel. **(b)** Box-whisker plots of the NH_3 concentration sampled at each site, setting 20 as the breaking point of *y* axis. The box boundaries represent the 25th and 75th percentile, the horizontal line is the median, and the whiskers mark the 10th and 90th percentiles. **(c)** Relationship between the NH_3 concentration at T-d (the exit of the Handan tunnel) and the other four sites varying in distance from the Handan road in the open environment.

ACPD
15, 34719–34763, 2015